Cell

TRP Channel Regulates EGFR Signaling in Hair Morphogenesis and Skin Barrier Formation

Xiping Cheng,[1,8] Jie Jin,[2,3,8] Lily Hu,[1] Dongbiao Shen,[1] Xian-ping Dong,[1] Mohammad A. Samie,[1] Jayne Knoff,[1] Brian Eisinger,[1] Mei-ling Liu,[1] Susan M. Huang,[4] Michael J. Caterina,[4] Peter Dempsey,[5] Lowell Evan Michael,[6] Andrzej A. Dlugosz,[6] Nancy C. Andrews,[2,7] David E. Clapham,[3,*] and Haoxing Xu[1,3,*]

[1]The Department of Molecular, Cellular, and Developmental Biology, the University of Michigan, 3089 Natural Science Building (Kraus), 830 North University, Ann Arbor, MI 48109, USA

[2]Division of Hematology and Oncology, Children's Hospital Boston, Karp Family Building 8-125A, Boston, MA 02115, USA

[3]The Department of Cardiology, Children's Hospital Boston, Manton Center for Orphan Disease, Enders 1350, 320 Longwood Avenue, Boston, MA 02115, USA

[4]Department of Biological Chemistry and Department of Neuroscience, Johns Hopkins University School of Medicine, Baltimore, MD 21025, USA

[5]The Department of Pediatrics and Communicable Diseases and Department of Molecular & Integrative Physiology, the University of Michigan, 1500 East Medical Center Drive, Room D3252, Ann Arbor, MI 48109, USA

[6]The Department of Dermatology and Comprehensive Cancer Center, the University of Michigan, 1500 East Medical Center Drive, Ann Arbor, MI 48109, USA

[7]Department of Pediatrics and Department of Pharmacology and Cancer Biology, Duke University School of Medicine, DUMC 2927, Durham, NC 27710, USA

[8]These authors contributed equally to this work

*Correspondence: dclapham@enders.tch.harvard.edu (D.E.C.), haoxingx@umich.edu (H.X.)

DOI 10.1016/j.cell.2010.03.013

SUMMARY

A plethora of growth factors regulate keratinocyte proliferation and differentiation that control hair morphogenesis and skin barrier formation. Wavy hair phenotypes in mice result from naturally occurring loss-of-function mutations in the genes for TGF-α and EGFR. Conversely, excessive activities of TGF-α/EGFR result in hairless phenotypes and skin cancers. Unexpectedly, we found that mice lacking the *Trpv3* gene also exhibit wavy hair coat and curly whiskers. Here we show that keratinocyte TRPV3, a member of the *t*ransient *r*eceptor *p*otential (TRP) family of Ca^{2+}-permeant channels, forms a signaling complex with TGF-α/EGFR. Activation of EGFR leads to increased TRPV3 channel activity, which in turn stimulates TGF-α release. TRPV3 is also required for the formation of the skin barrier by regulating the activities of transglutaminases, a family of Ca^{2+}-dependent crosslinking enzymes essential for keratinocyte cornification. Our results show that a TRP channel plays a role in regulating growth factor signaling by direct complex formation.

INTRODUCTION

Skin and its appendages provide a protective barrier essential for animal survival. Hair morphogenesis and epidermal development are orchestrated by an array of cytokines and growth factors (Fuchs and Raghavan, 2002). Signaling by these diffusible molecules provides spatially and temporally controlled cellular programs for keratinocyte proliferation, differentiation, migration, and finally, terminal differentiation and cornification. TGF-α and epidermal growth factor (EGF) are related autocrine/paracrine growth factors that activate the EGF receptor (EGFR; ErbB1) to regulate the balance between keratinocyte proliferation and differentiation (Schneider et al., 2008). Defective TGF-α/EGFR signaling leads to abnormal hair morphogenesis, manifested by the "wavy hair" and "curly whiskers" phenotypes of spontaneous loss-of-function mouse mutations in TGF-α (named *waved-1* or *wa1*) and in EGFR (named *waved-2* or *wa2*), respectively (Ballaro et al., 2005; Luetteke et al., 1993, 1994; Mann et al., 1993; Murillas et al., 1995; Schneider et al., 2008; Sibilia and Wagner, 1995; Threadgill et al., 1995). Excessive activities of TGF-α/EGFR cause a hairless phenotype and skin cancers (Ferby et al., 2006; Schneider et al., 2008). The mechanisms by which TGF-α/EGFR signaling determines cell fate (proliferation versus differentiation) of follicular and interfollicular (epidermal) keratinocytes are not completely understood.

Accumulated evidence suggests that both negative and positive feedback mechanisms coexist in the TGF-α/EGFR signaling axis. EGF binding triggers rapid degradation of the EGFR through endocytic pathways but also leads to further production and release/shedding of TGF-α/EGF (Coffey et al., 1987; Peschon et al., 1998). This unique autoinduction mechanism may contribute to the effects of TGF-α/EGF on keratinocyte terminal differentiation (Peus et al., 1997; Sakai et al., 1994;

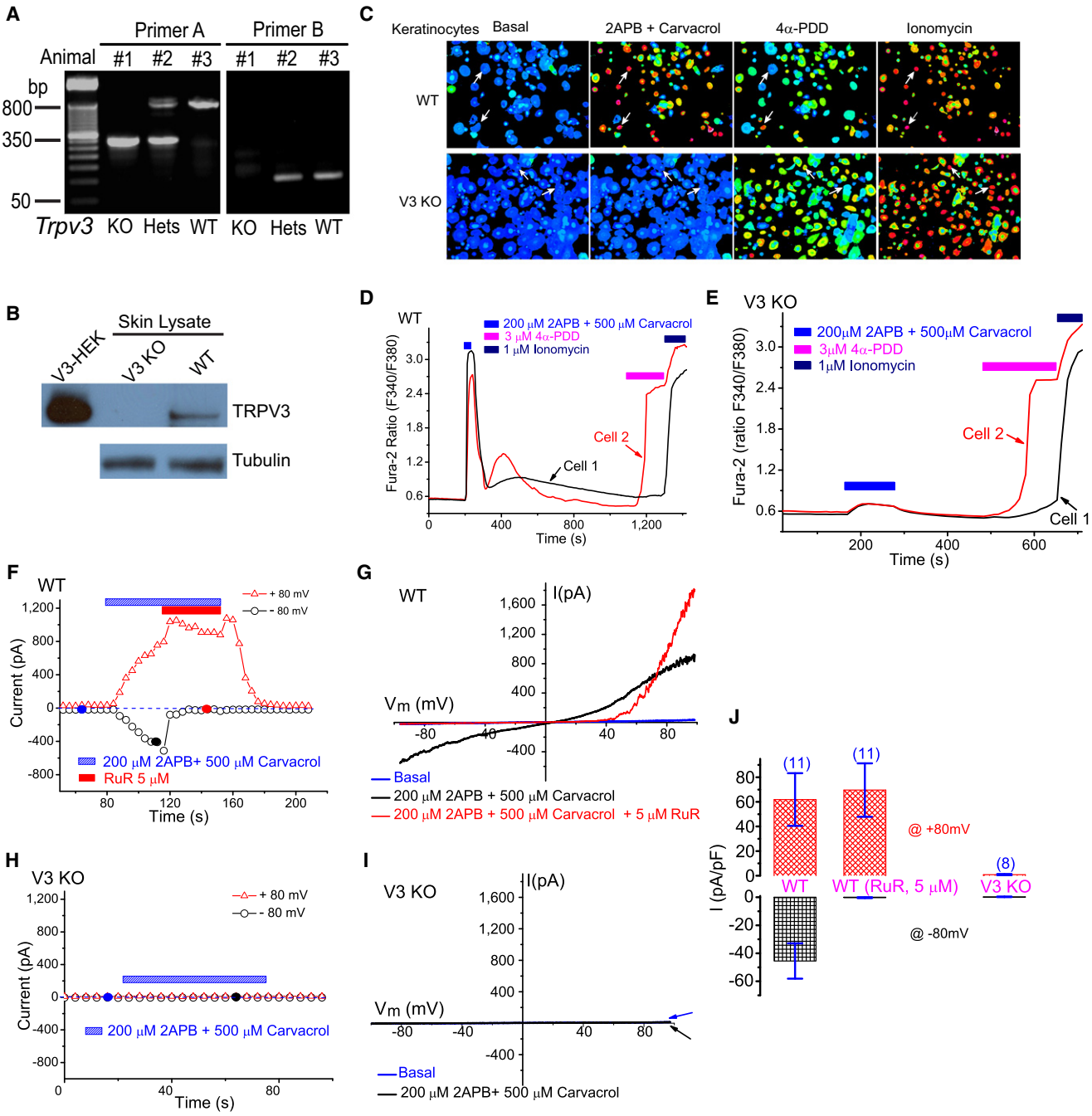

Figure 1. Targeted Deletion of Mouse *Trpv3* Abolishes the Response of Keratinocytes to TRPV3 Activators

(A) PCR genotyping of wild-type (WT), V3 KO, and heterozygous (Hets) mice. Two sets of primers were used as described in Experimental Procedures. PCR products for primer set A: WT 800 bp, KO 300 bp. For primer set B: WT 130 bp, KO no product.

(B) Lack of TRPV3 protein expression in the skin of V3 KO mice. TRPV3 was immunoprecipitated and immunoblotted using a TRPV3-specific monoclonal antibody. Cell lysates from HEK293T cells expressing recombinant mouse TRPV3 (V3-HEK) were used as positive controls. γ-Tubulin served as a loading control for skin lysates.

(C–E) Lack of agonist-induced V3-like Ca^{2+} response in V3 KO primary keratinocytes. (C) TRPV3 agonist cocktail (200 μM 2-APB + 500 μM Carvacrol) induced large increases of $[Ca^{2+}]_i$ in primary cultured keratinocytes isolated from WT ($V3^{+/+}$) but not V3 KO ($V3^{-/-}$) mice. Whereas more than 80% of WT keratinocytes responded strongly to the V3 agonist cocktail, negligible responses were observed for V3 KO keratinocytes. Positive controls: ~60%–80% keratinocytes from both genotypes (WT and V3 KO) responded to 4α-PDD (3 μM; agonist of TRPV4). All cells responded to ionomycin (1 μM). (D) Ca^{2+} responses of two representative WT cells from (C) (arrows; upper panels). One cell responded to both TRPV3 and TRPV4 agonists whereas the other one only responded to the V3 agonist cocktail. (E) Ca^{2+} responses of two representative V3 KO cells from (C) (arrows; lower panels). One cell responded to the TRPV4 agonist (cell 2); neither cell responded significantly (<0.1 fura-2 ratio) to the V3 agonist cocktail.

Schneider et al., 2008). TGF-α is expressed in both basal (proliferating) and suprabasal (differentiating) layers of epidermis and in the inner root sheath of the hair follicle (Coffey et al., 1987; Luetteke et al., 1993; Mann et al., 1993; Schneider et al., 2008). Although most highly expressed in the basal layer, suprabasal keratinocytes also express EGFR (Luetteke et al., 1993; Mann et al., 1993; Schneider et al., 2008). Although induction of differentiation dramatically increases the production of TGF-α/EGF (Denning et al., 2000), these same growth factors promote terminal differentiation (Wakita and Takigawa, 1999).

Previous studies suggest that TGF-α/EGF regulate keratinocyte terminal differentiation likely in a Ca^{2+}-dependent manner (Denning et al., 2000; Sakai et al., 1994). Intracellular Ca^{2+} regulates both expression and shedding from the membrane-tethered precursors of EGFR ligands (Denning et al., 2000; Horiuchi et al., 2007). Ca^{2+} ionophores are sufficient to induce both production and release of TGF-α (Horiuchi et al., 2007; Pandiella and Massague, 1991). The Ca^{2+} influx pathway under physiological conditions, however, has not been identified.

The cornified cell envelope (CE) is a protein-lipid layer that replaces the plasma membrane of terminally differentiated keratinocytes (corneocytes) and is crucial for the stratum corneum epidermal barrier (Lorand and Graham, 2003). The CE is a complex layer of lipids attached to a layer of crosslinked proteins. The transglutaminases (TGases) primarily form ε-(γ-glutamyl) lysine isopeptide bonds between proteins, and their activities strongly depend on intracellular Ca^{2+} levels (Lorand and Graham, 2003). EGF can acutely activate TGases to induce CE formation and keratinocyte terminal differentiation (Lorand and Graham, 2003). Cornification-promoting cellular cues may activate an unidentified Ca^{2+} influx channel to induce TGase activity and subsequent CE formation.

*T*ransient *r*eceptor *p*otential (TRP) proteins are a large family of Ca^{2+}-permeable channels with diverse functions (Montell, 2005; Nilius et al., 2007; Ramsey et al., 2006). Among these, TRPV3 and TRPV4 are functionally expressed in keratinocytes (Chung et al., 2004; Moqrich et al., 2005). These channels detect ambient temperature changes and are activated by various plant-derived and synthetic compounds (Moqrich et al., 2005; Xu et al., 2006). In this study, we find that TRPV3-deficient mice exhibit hair phenotypes similar to *wa1* and *wa2*. Molecular and biochemical analyses of TRPV3-deficient mice and isolated keratinocytes reveal defective TGF-α/EGFR signaling. We propose that TRPV3 is a Ca^{2+} entry pathway tightly associated with the TGF-α/EGFR signaling complex orchestrating keratinocyte terminal differentiation.

RESULTS

Whole-Animal and Keratinocyte-Specific Disruption of Mouse *Trpv3* Gene

Using a recombineering method, we inserted two loxP sites to flank exon 13 of mouse *Trpv3* (see Figure S1 available online) and obtained mice with homozygous floxed (fl) alleles. To investigate the in vivo function(s) of TRPV3, we generated TRPV3 global knockout (KO) using Sox2-Cre transgenic mice (details described in Experimental Procedures). To elucidate the role of TRPV3 in the skin, we also bred the fl/fl animals to mice harboring a *K14-Cre* recombinase transgene, which efficiently expresses Cre throughout the epidermis by embryonic day 15.5 (E15.5) (Wang et al., 1997). Mouse genotypes from both TRPV3 global KO (*Trpv3*$^{-/-}$; abbreviated as V3 KO) and K14-specific conditional KO (V3 fl/fl: K14 Cre; abbreviated as V3 cKO) were confirmed by PCR (Figure 1A, also see Figure S1). No TRPV3 full-length transcript was detected from V3 KO skin tissues using RT-PCR analysis (Figure S1). No full- length TRPV3 protein was detected by western blot in V3 KO skin lysates (Figure 1B) or cultured primary keratinocytes (data not shown). Thus, the mice generated completely lack TRPV3 in their skin.

Functional Characterization of TRPV3 Global and Keratinocyte-Specific KO Mice

We performed functional studies in keratinocytes isolated from V3 KO and control (wild-type [WT], V3$^{+/+}$; heterozygous or Hets, V3$^{+/-}$) mice. Fura-2 Ca^{2+} imaging was employed to study the response of keratinocytes to TRPV3 chemical agonists (Xu et al., 2006). Application of most TRPV3 agonists alone, for example, 2-APB (200 μM) or Carvacrol (500 μM), induced a small increase in intracellular Ca^{2+} ($[Ca^{2+}]_i$) in a subset of cells (30% to 80% of cells; data not shown). However, coapplication of two agonists, for example, 200 μM 2-APB + 500 μM Carvacrol (TRPV3 agonist cocktail), reliably induced a dramatic (ΔF340/F380 > 1) increase of $[Ca^{2+}]_i$ in the majority (>80%) of keratinocytes isolated from WT mice (WT keratinocytes; Figures 1C and 1D). Similar results were obtained for other combinations of TRPV3 agonists such as 200 μM 2-APB + 5 mM Camphor; removal of external Ca^{2+} abolished most of the agonist-induced Ca^{2+} responses. No significant increase (ΔF340/F380 < 0.1) in $[Ca^{2+}]_i$ was seen in keratinocytes isolated from V3 KO mice (V3 KO keratinocytes; Figures 1C and 1E). In contrast, in both WT and V3 KO cells, large $[Ca^{2+}]_i$ increases were evoked by 4α-PDD (3 μM), an agonist of TRPV4 (Watanabe et al., 2002) that is also expressed in keratinocytes. Similar results were

(F–J) TRPV3-like currents were completely absent in V3 KO primary keratinocytes. (F) Application of the V3 agonist cocktail (200 μM 2-APB + 500 μM Carvacrol) to WT primary keratinocytes induced TRPV3-like (I_{TRPV3}) currents. Whole-cell currents were generated in response to 400 ms voltage ramps from −100 to +100 mV, applied every 4 s. Holding potential = 0 mV. Each symbol represents the current amplitude at +80 mV (red triangles) and −80 mV (black circles), respectively. Blue dashed line = zero current. (G) Representative ramp current of I_{TRPV3}. I-V relations were recorded at time points noted in (H) (filled circles). I_{TRPV3} was doubly rectifying and reversed near 0 mV. Ruthenium red (RuR; 5 μM) selectively blocked inward I_{TRPV3} with significant augmentation at very positive potentials. (H and I) No significant currents were induced by the V3 agonist cocktail in V3 KO keratinocytes. (J) Average I_{TRPV3} current densities elicited by the V3 agonist cocktail alone or with the coapplication of RuR (5 μM). At −80 mV, inward I_{TRPV3} of WT keratinocytes were −45 ± 13 pA/pF (n = 11) and −0.3 ± 0.3 pA/pF (n = 11) in the absence or presence of RuR, respectively. At +80 mV, outward I_{TRPV3} of V3$^{+/+}$ keratinocytes were 62 ± 21 pA/pF (n = 11) and 70 ± 21 pA/pF (n = 11) in the absence or presence of RuR, respectively. For V3 KO keratinocytes, no significant inward or outward I_{TRPV3} was detected: −0.3 ±± 0.3 pA/pF at −80mV (n = 8) and 0.8 ± 0.5 pA/pF at +80 mV (n = 8), respectively.

Data are presented as the mean ± standard error of the mean (SEM). See also Figure S1.

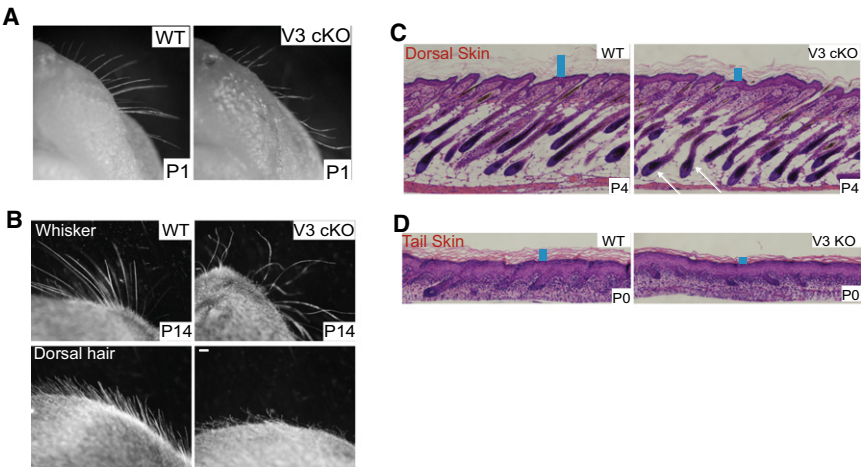

Figure 2. TRPV3-Deficient Mice Exhibit Curly Whiskers, Wavy Hair, Misaligned Hair Follicles, and a Thin Stratum Corneum

(A) Newborn (P1) V3 cKO (fl/fl: K14 Cre) mice: curly whiskers; littermate WT (V3 fl/fl) animals: straight whiskers.

(B) Whiskers in an adult WT mouse (P14) were straight; the whiskers of littermate V3 cKO mice were distinctively curly and hooked (upper panels). V3 cKO mice also exhibited wavy dorsal coats (lower panels).

(C and D) Skin and hair follicle abnormalities of V3-deficient mice revealed by H&E staining of dorsal (C) and tail (D) skin sections from WT and KO or cKO mice. In the back skin of WT pups (P4), all hair follicles lay parallel in an anterior to posterior direction with an angle of ~45° (left panel). In contrast, hairs of littermate cKO mice angled in different directions (right panel). Arrows indicate two misaligned horizontally oriented hair follicles. In addition to the hair follicle abnormality, the stratum corneum (SC) layer (denoted by blue rectangle bars) of the V3 KO or cKO mice was significantly thinner but more compact than that of the WT mice.

See also Figure S2.

obtained in keratinocytes from V3 cKO mice. These results demonstrate that TRPV3 KO mouse keratinocytes completely lack TRPV3-mediated Ca^{2+} responses.

Consistent with the Ca^{2+} imaging results, TRPV3 agonist cocktail evoked a slowly developing, large TRPV3-like current (I_{TRPV3}) in most WT keratinocytes (Figures 1F, 1G, and 1J). Ruthenium red (RuR, 5 μM), a nonspecific voltage-dependent blocker of TRPV1-4 channels (Chung et al., 2004; Hu et al., 2004; Ramsey et al., 2006; Xu et al., 2006), almost completely (>99%) inhibited agonist-activated inward I_{TRPV3}. Similar RuR-sensitive I_{TRPV3} was also evoked by other TRPV3 agonists (200 μM 2-APB + heat or 200 μM 2-APB + 5 mM Camphor) in the same cells. In V3 KO keratinocytes, in contrast, no significant current was evoked by the V3 agonist cocktail (Figures 1H, 1I, and 1J). Similar results were obtained in keratinocytes from V3 cKO mice.

TRPV3-Deficient Mice Exhibit Curly Whiskers and Wavy Hair

Although previous animal studies identified TRPV3's function in temperature sensation (Moqrich et al., 2005), the most obvious phenotypic changes we observed from our V3 KO mice are abnormalities in skin, hair, and whiskers. In contrast with littermate controls (WT and heterozygotes [Hets]), most whiskers of V3 KO mice were characteristically curled or hooked (Figure S2). The curly morphology of whiskers was apparent at birth (Figure S2); newborn V3 KO mice could be identified based on whisker morphology alone. Keratinocyte-specific V3 cKO mice exhibited similar curly whiskers (Figures 2A and 2B), suggesting that the phenotype was caused by specific V3 deficiency in keratinocytes. Whisker curliness grew more obvious with age (Figure 2B and Figure S2). Both the dorsal and ventral coat fur, as well as the tail hair, of V3 KO and cKO mice were wavy (Figure 2B and Figure S2) beginning 1 week after birth but was most apparent once the hair was well formed (~3–4 weeks postnatal), gradually reducing with age. In contrast to a previous study reporting abnormality of ventral hairs in a subset of V3 KO mice (Moqrich et al., 2005), curly whiskers and wavy hair were present throughout the coat at all ages with 100% penetrance for both V3 KO and cKO mice that we have generated, as well as the V3 KO mice reported by Moqrich et al. (H.L., S.M.H., and M.J.C., unpublished data). In comparison, TRPV1 KO mice hair shape and distribution are normal (Figure S2). Consistent with the expression of TRPV3 in follicular keratinocytes of mouse (Peier et al., 2002) and human (Xu et al., 2002), the wavy phenotype correlated with V3 deficiency in keratinocytes.

Skin contains many cell types, including sensory nerves. However, as the K14 promoter drives the expression of Cre recombinase specifically in all keratinocytes (both follicular and interfollicular) in the skin (Coulombe et al., 1989), the results obtained from V3 cKO, V3 fl/fl: K14 Cre mice suggested that the defect in hair morphogenesis was due to the lack of TRPV3 expression in keratinocytes in a cell-autonomous manner. Both hair and whisker phenotypes were independent of pigmentation of the hair and genetic background, as black-coated (C57BL/6) backcrossed (>6 generations) V3 KO mice displayed phenotypes similar to those of mice with mixed genetic background (BL6 and 129sv) (Figure S2). V3 KO pups were born with the expected Mendelian ratio, and body weight was comparable to control mice (Figure S2).

In histological examinations of skin from the mid-dorsal region of mice of different ages, we found that a subset of hair follicles exhibited an obvious but gentle curvature (Figure S2). In Haematoxylin & Eosin (H&E) stained skin sections from control mice (P4), hair follicle shafts were parallel and posed roughly at a 45° angle to the subcutaneous muscle layer (Figure 2C). In contrast, individual hair follicles of V3 cKO mice were, in many cases, gently curved and pointed in different directions with variable

angles (Figure 2C). Several hair follicles even grew horizontally to the subcutaneous muscle layer. Similar follicular derangement was obvious for V3 KO mice (Figure S2). Notably, similar alterations in hair follicle morphology have been reported in EGFR-deficient mice (Threadgill et al., 1995). These results suggest that the wavy hair phenotype of V3 KO mice was due to a defect in follicle formation, and that mouse TRPV3 was required for normal morphogenesis of hair and whiskers. In addition to follicular abnormalities, V3 KO and cKO mice also exhibited abnormalities in the epidermal stratum corneum (Figures 2C and 2D; Figure S2; details see below). The hair cycle, however, was not significantly altered (Figure S2).

Defective TGF-α/EGFR Signaling in TRPV3-Deficient Mice

The hair and whisker phenotype of V3 KO mice resembled largely those of *wa1* and *wa2* mice, as well as other mouse mutations with reduced expression/release/activity in TGF-α and/or EGFR (Ballaro et al., 2005; Du et al., 2004; Luetteke et al., 1993, 1994; Mann et al., 1993; Miettinen et al., 1995; Murillas et al., 1995; Peschon et al., 1998; Schneider et al., 2008; Sibilia and Wagner, 1995; Threadgill et al., 1995) (see Figure S3). Thus we investigated whether TGF-α and/or EGFR signaling was altered in V3 KO mice. Real-time semiquantitative PCR (q-PCR) analysis of the skin of V3 KO pups revealed that the mRNA expression level of TGF-α was half that of WT (P4; Figure 3A). TGF-α mRNA levels of newborn (P0) V3 KO animals, though significantly less than those of the P4 mice, were comparable to those of the littermate controls (P0). Expression (mRNA) levels of several other EGFR ligands and EGFR (Figure S3), however, were not significantly altered in the skin of V3 KO mice. These results suggest that TRPV3 affects the expression level of TGF-α in postnatal skin in vivo.

Both expression and proteolytic shedding of the membrane-tethered TGF-α are known to be Ca^{2+} dependent (Denning et al., 2000; Horiuchi et al., 2007). We used an ELISA assay optimized for human TGF-α to investigate the role of TRPV3 in TGF-α shedding/release. In the presence of TRPV3 agonist cocktail (100 μM 2-APB + 250 μM Carvacrol; 30 min), normal human epidermal keratinocytes (NHEK) released more than twice the amount of TGF-α into the culture medium. This is comparable to the effect of PMA, a stimulus well known to induce release and expression of TGF-α (Figure 3B). ADAM17, the principal sheddase required for TGF-α release (Peschon et al., 1998), was required for V3 agonist-induced TGF-α release/shedding (Figure 3C).

As the level of TGF-α was reduced in V3 KO skin, one would expect that its activated receptor, phosphorylated EGFR (P-EGFR), might also be reduced. By immunoblot analysis of P-EGFR in skin lysates of V3 KO skin, EGFR activity was only about one-third of that of WT controls (Figures 3D and 3E). Interestingly, the expression level of total EGFR was slightly but significantly increased in V3 KO skin (1.8- ± 0.3-fold, n = 6), so that the ratio of P-EGFR/total EGFR was about 5-fold less (0.20 ± 0.03, n = 4) in V3 KO skin. This level of the reduction was comparable to those of the hypofunctional EGFR mutations causing "wavy" phenotypes (Du et al., 2004). Consistent with biochemical results, EGFR staining was more prominent in V3 KO frozen skin sections (Figure S3), whereas P-EGFR immunostaining was weaker. These results are consistent with dramatically reduced EGFR activity in V3 KO mice and suggest that the level of total EGFR was increased as a consequence of reduced activity, tyrosine phosphorylation-dependent endocytic degradation (Schneider et al., 2008), or other compensatory mechanisms. The reduction of EGFR activity in V3 KO mice was probably due to the loss of the TRPV3 channel activity, as activation of TRPV3 in cultured keratinocytes using TRPV3 agonists resulted in increases in both TGF-α release (Figures 3B and 3C) and EGFR activity (Figure 3F and Figure S3). Notably, the TRPV3-induced increase of EGFR activity in keratinocytes was abolished by a neutralizing TGF-α antibody or ADAM17 sheddase inhibitor (Figures 3F and 3G), suggesting that activation of TRPV3 led to an increase in TGF-α release and subsequent EGFR activation.

Regulation of TRPV3 Channel Activity by TGF-α/EGFR Signaling

Several in vitro studies provided evidence that TRP channels are regulated by members of the receptor tyrosine kinase (RTK) family (Li et al., 1999; Ramsey et al., 2006). We hypothesized that TRPV3 channel activity could also be upregulated by EGFR signaling. In serum-starved primary keratinocytes cultured in the absence of TGF-α, Ca^{2+} responses could be induced by a high concentration (100 μM 2-APB + 250 μM Carvacrol), but not by a lower concentration (50 μM 2-APB + 125 μM Carvacrol), of V3 agonist cocktail (Figures 4A and 4C). In the presence of TGF-α (100 ng/ml for 3–5 hr), however, large $[Ca^{2+}]_i$ increases were recorded even with a low concentration (50 μM 2-APB + 125 μM Carvacrol) of V3 agonist cocktail; responses to a high concentration of V3 agonists were comparable to those without TGF-α treatment (Figures 4B and 4C). Similar results were seen with EGF (100 ng/ml) pretreatment (Figure S4). TGF-α/EGF treatment altered the sensitivity of TRPV3 in keratinocytes to V3 agonists, suggesting that the increased activity was at least partially mediated by increased channel gating, rather than the expression or surface expression of TRPV3 proteins. Consistent with this interpretation, the temperature-induced response (from 22°C to 41°C) was also significantly larger in TGF-α-treated keratinocytes (Figure S4). The sensitizing effect of TGF-α was most likely mediated by EGFR, as an EGFR inhibitor (AG1478) or shRNA knockdown of EGFR expression (Figure S4) completely or largely eliminated its potentiation (Figures 4D and 4E). Because inhibitors of PLC (U73122) and ERK (PD98059) completely or partially blocked potentiation (Figure 4D), these pathways may underlie the sensitizing effect downstream of EGFR receptor activation. In support of this finding, shRNA knockdown of PLC-γ1 expression (Figure S4) significantly decreased the sensitizing effect of TGF-α (Figure 4E). Consistent with our $[Ca^{2+}]_i$ measurements, I_{TRPV3} exhibited a similar dependence on TGF-α (Figure 4F).

The results presented so far raise the possibility that TRPV3 and EGFR might be in a signaling complex. To test this hypothesis, coimmunoprecipitation (co-IP) experiments were first performed in a heterologous expression system. In cells transfected with TRPV3, either alone or together with EGFR, both endogenous (data not shown) and overexpressed EGFR (Figure S4) were found to co-IP with TRPV3. Next, we confirmed this finding

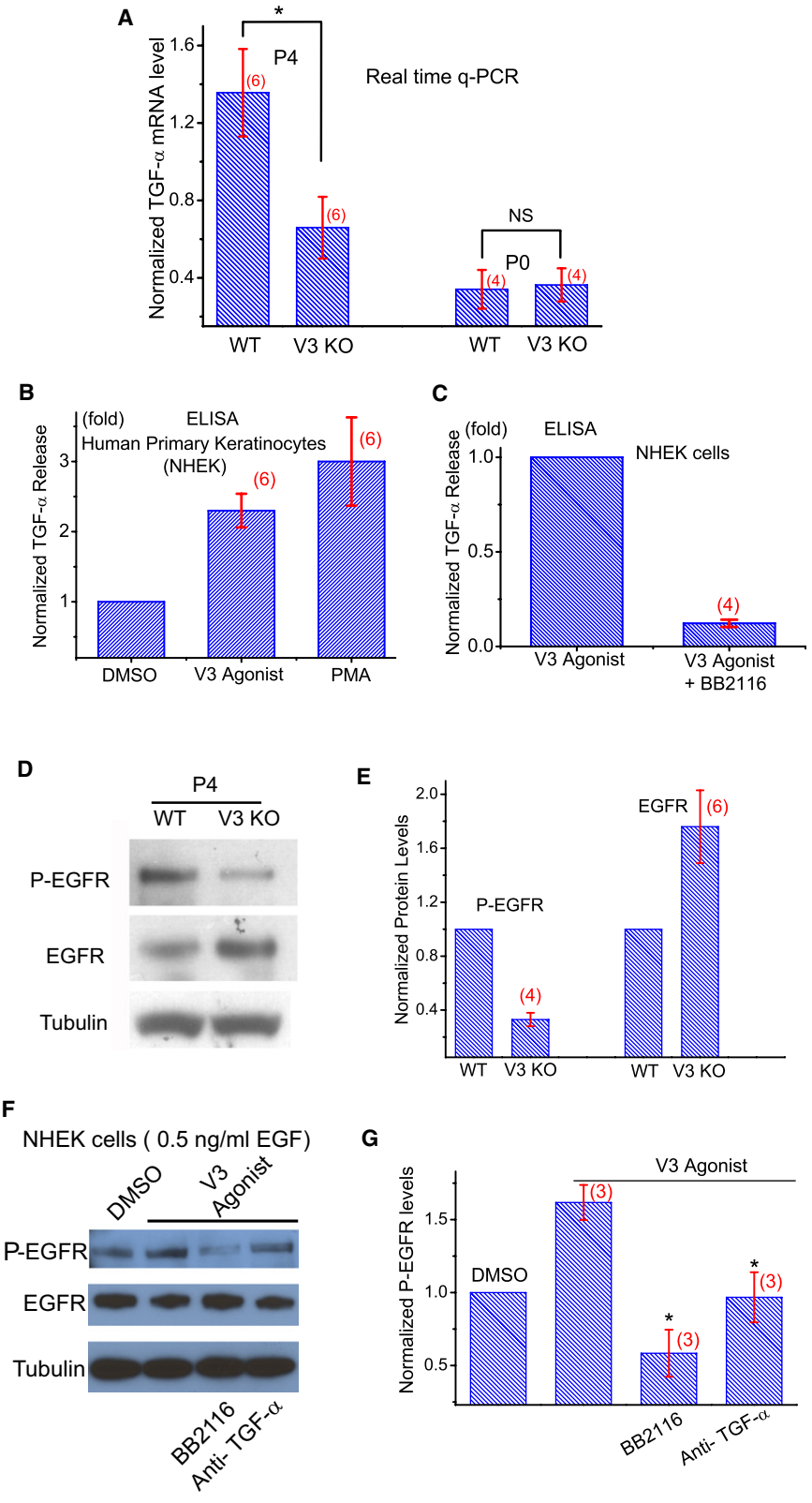

Figure 3. Reduced Levels of TGF-α and Decreased Activity of EGFR in the Skin of TRPV3-Deficient Mice

(A) mRNA expression levels (q-PCR) of TGF-α were significantly ($p < 0.05$) lower in V3 KO skin tissues from P4 but not P0 mice.

(B) Short application of V3 agonist cocktail (100 μM 2-APB + 250 μM Carvacrol; 30 min) significantly increased TGF-α release into the culture medium from primary human keratinocytes (NHEK). TGF-α was measured with ELISA; PMA was used as a positive control.

(C) V3 agonist-induced TGF-α release was diminished in the presence of BB2116 (20 μM), an inhibitor of ADAM17 required for the shedding of TGF-α.

(D) Immunoblotting analysis of phosphorylated (active; P-EGFR) and total EGFR expression levels of WT and V3 KO skin lysates. Compared to WT mice, the level of P-EGFR was significantly decreased in V3 KO skin lysates. In contrast, the expression level of total EGFR was slightly but significantly increased in V3 KO skin lysates.

(E) Statistical analyses of EGFR and P-EGFR expression levels.

(F and G) EGFR activity (P-EGFR) was enhanced by V3 agonist cocktail (100 μM 2-APB + 250 μM Carvacrol) for 30 min. The basal activation of EGFR was induced by a minimal concentration of EGF (0.5 ng/ml). The enhancement was abolished in the presence of BB2116 (20 μM) or a neutralizing antibody against TGF-α (1 μg/ml).

Data in (A), (B), (C), (E), and (F) are presented as the mean ± SEM. See also Figure S3.

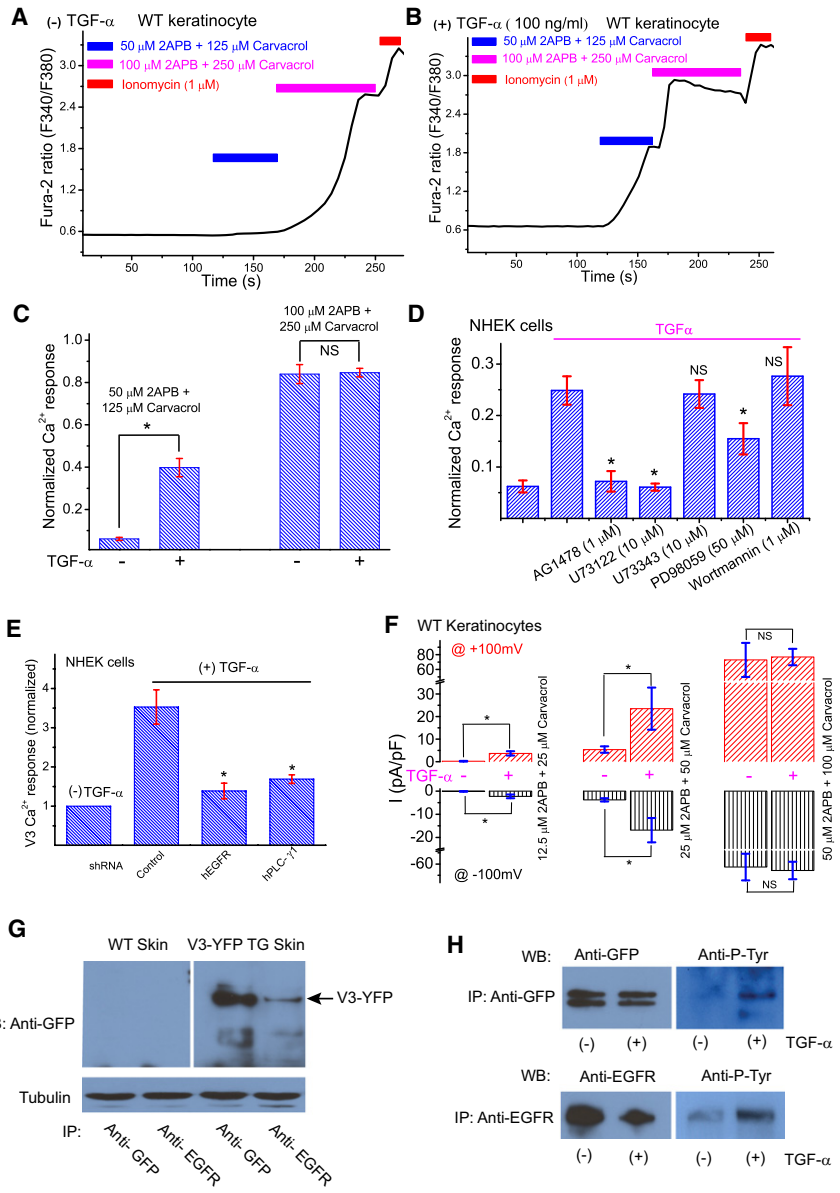

Figure 4. Activation of EGFR Increases TRPV3 Channel Activity in Cultured Primary Keratinocytes

(A) Weak V3 Ca^{2+} responses were seen in serum-starved keratinocytes without TGF-α treatment. A representative WT keratinocyte failed to respond significantly to a low concentration of V3 agonist cocktail (50 μM 2-APB + 125 μM Carvacrol). A higher concentration of V3 agonist cocktail (100 μM 2-APB + 250 μM Carvacrol), however, induced a significant increase of $[Ca^{2+}]_i$ in the same cell.

(B) A representative keratinocyte that was pretreated with TGF-α (100 ng/ml) for 3 hr showed a significant response to a low concentration of V3 agonist cocktail (50 μM 2-APB + 125 μM Carvacrol). A larger increase in $[Ca^{2+}]_i$ was seen with a higher concentration of V3 agonist cocktail (100 μM 2-APB + 250 μM Carvacrol).

(C) Average V3 Ca^{2+} responses in mouse keratinocytes with and without TGF-α pretreatment.

(D) EGFR mediates the sensitizing effect of TGF-α in human primary keratinocytes in a PLC-dependent manner. TGF-α (100 ng/ml) pretreatment significantly increased V3 Ca^{2+} response (by low concentration of V3 agonist cocktail) in NHEK keratinocytes. In the presence of AG1478 (1 μM; an inhibitor of EGFR) or U73122 (10 μM, a PLC inhibitor), TGF-α failed to increase agonist-induced V3 Ca^{2+} responses. Partial inhibition was seen in cells treated with ERK inhibitors.

(E) ShRNA-mediated knockdown of EGFR or PLC-γ1 abrogates the sensitizing effect of TGF-α in human primary keratinocytes.

(F) TGF-α pretreatment significantly increased V3 current in keratinocytes in response to a low concentration but not at high concentrations of V3 agonists.

(G) Coimmunoprecipitation of TRPV3 and EGFR in skin tissues from V3-YFP transgenic mice. Immunoprecipitates (IP) were formed with the indicated antibodies and visualized on western blot (WB). TRPV3-YFP was recognized by monoclonal anti-GFP; TRPV3-YFP band is indicated by arrow. EGFR was IP'd by polyclonal anti-EGFR.

(H) TGF-α-induced tyrosine phosphorylation of TRPV3 in HEK293 cells. HEK293 cells were transiently transfected with the cDNAs of TRPV3-GFP and EGFR and treated with, or without, TGF-α (100 ng/ml) as shown. TRPV3-GFP was IP'd by a monoclonal anti-GFP and WB'd by a pan-phosphotyrosine antibody. EGFR was IP'd by polyclonal anti-EGFR and WB'd by a pan-phosphotyrosine antibody.

Data in (C)–(F) are presented as the mean ± SEM. See also Figure S4.

in keratinocytes (Figure 4G) using skin tissues from TRPV3-YFP transgenic mice (Huang et al., 2008). These results suggest that EGFR can directly or indirectly associate with TRPV3 in both heterologous and native systems. Consistent with the close association of these molecules, we found that activation of EGFR with TGF-α resulted in tyrosine phosphorylation of TRPV3 (Figure 4H).

Altered Keratinocyte Differentiation in TRPV3-Deficient Mice

EGFR signaling is known to have at least two distinct functions in epidermis (Schneider et al., 2008). In the basal layer, TGF-α/EGFR signaling promotes keratinocyte proliferation (Schneider et al., 2008). The function of EGFR signaling in suprabasal cells is to promote late terminal differentiation (Ballaro et al., 2005; Dlugosz et al., 1994; Peus et al., 1997; Wakita and Takigawa, 1999). Whereas proliferating keratinocytes in the basal layer express structural keratins K5/K14, differentiating keratinocytes express the structural keratins K1/K10 (Byrne et al., 2003). As keratinocytes move closer to the skin surface, expression of K1/K10 declines and loricrin expression increases (Byrne et al., 2003), as they undergo cornification. Consistent with previous studies (Wakita and Takigawa, 1999), we observed that EGF significantly reduced the expression of the early differentiation marker K1 in suspended keratinocytes (Figure S5).

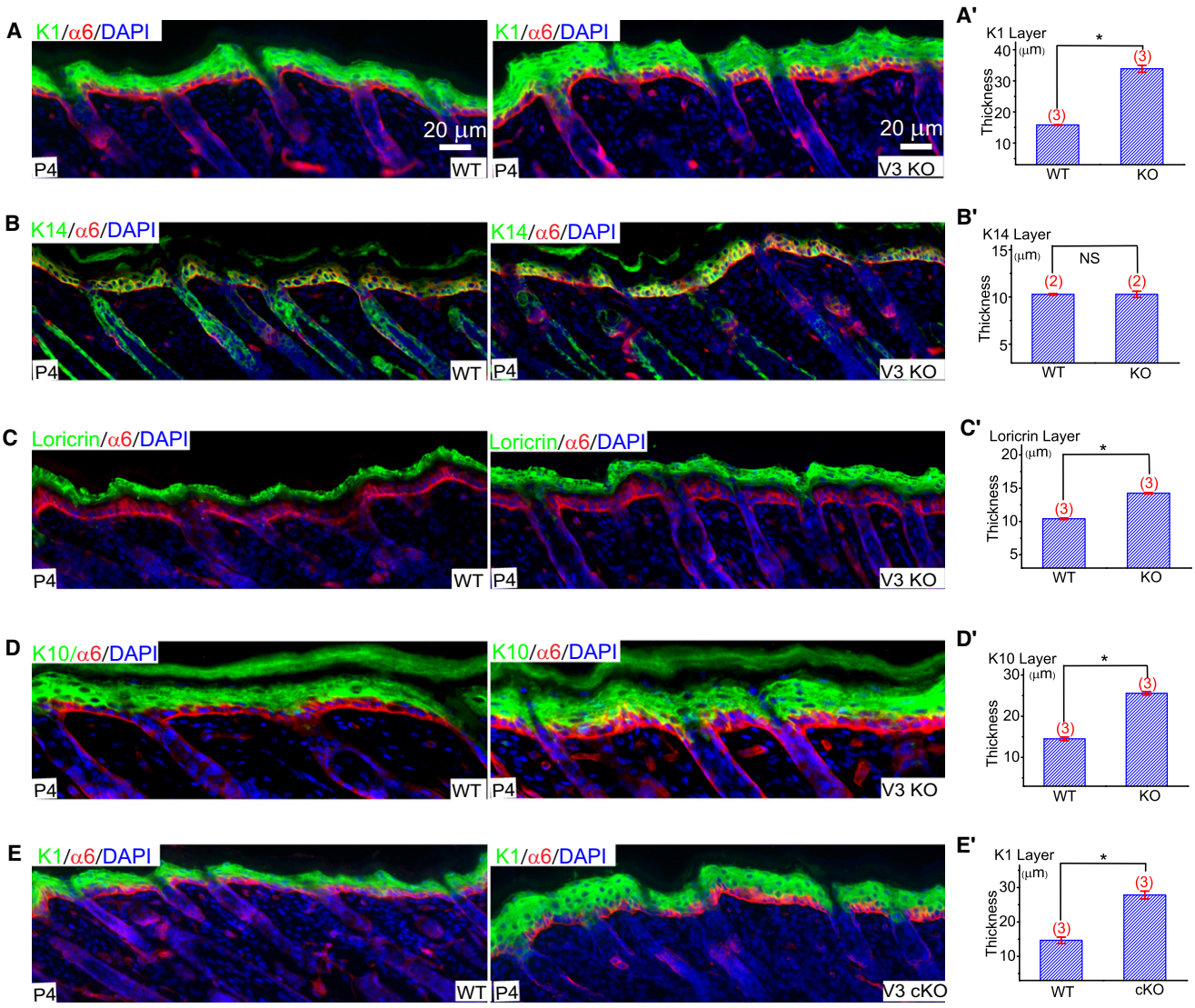

Figure 5. Genetic Inactivation of TRPV3 Results in Increased Expression of Early Epidermal Differentiation Markers in Skin

(A–E) Immunofluorescence analyses of frozen skin sections from P4 pups.

(A and A′) Compared to WT mice, the immunofluorescence of keratin protein 1 (K1; a keratinocyte structural protein and a marker for the differentiating spinous and granular layers) was elevated in V3 KO skin sections. Integrin α6 antibody labeled the basement membrane, the boundary between epidermis and dermis. DAPI is a nuclear marker. The K1-positive layer was 2-fold thicker in V3 KO epidermis (quantified in the A′ panel).

(B and B′) Normal immunofluorescence of keratin protein 14 (K14; a keratinocyte structural protein and a marker for the proliferating basal layer).

(C and C′) Slightly but significantly elevated loricrin (a marker for the differentiating granular layer) immunofluorescence in V3 KO epidermis.

(D and D′) Elevated keratin protein 10 (K10; a keratin protein associated with K1 immunofluorescence in V3 KO epidermis.

(E and E′) Elevated K1 immunofluorescence in V3 cKO epidermis.

Data in (A′)–(E′) are presented as the mean ± SEM. See also Figure S5.

We reasoned that a reduced rate of autonomous EGFR-dependent proliferation or terminal differentiation would accelerate keratinocyte early differentiation in V3 KO cells. Compared to WT skin sections, V3 KO epidermis exhibited a >2-fold increase in the thickness of the K1-positive layer (Figure 5A), whereas cell sizes and densities were normal (Figure S5). Similar results were reported in transgenic mice with defective TGF-α/EGFR signaling or keratinocytes cultured in the presence of EGFR inhibitors (Ballaro et al., 2005; Peus et al., 1997). No significant change was observed in the K14 layer of V3 KO epidermis (Figure 5B). Loricrin expression was relatively less elevated in V3 KO epidermis (Figure 5C). Consistent with the increased early differentiation in V3 KO epidermis, thickness of K10 (interaction partner of K1) layer also increased in V3 KO animals (Figure 5D). Finally, V3 cKO animals exhibited similar alterations in keratinocyte differentiation (Figure 5E).

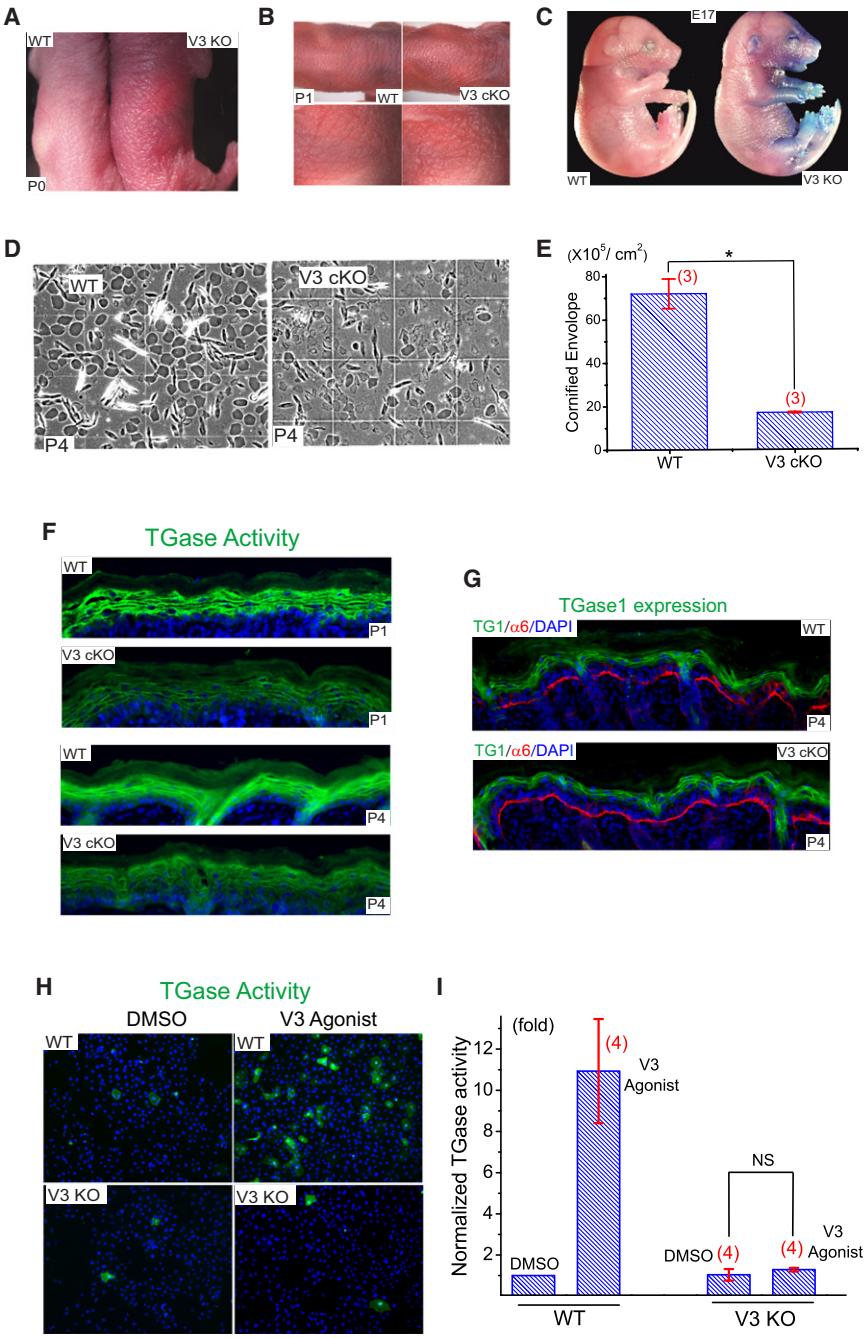

Figure 6. Defective Barrier Formation and Diminished TGase Activity in the Skin of TRPV3-Deficient Mice

(A) Compared to newborn (P0) WT mice (on the left), V3 KO skin was dry, reddened, and scaly.

(B) Similar dry and scaly skin was also seen in neonatal (P1) cKO mice.

(C) Toluidine blue dye exclusion assay of embryonic day 17 (E17) embryos. Staining indicates dye permeability and defective or immature barrier function. The upper and lower halves of the pictures were taken separately but shown in combination for the purpose of illustration.

(D and E) Compared to WT littermate pups (P4), the cornified cell envelopes (CEs) of skins of V3 cKO pups were significantly less mature.

(F) Compared to WT littermates, reduced TGase activity was detected in the frozen skin sections of neonatal (P1; upper two panels) V3 cKO mice. TGase activity was detected using an immunofluorescence-coupled in situ enzymatic assay. Positive staining was restricted to the granular layer of epidermis. Reduced TGase activity in the P4 (lower two panels) skin of V3 cKO.

(G) Expression levels of TGase1 were comparable for both WT and V3 cKO mice.

(H) Short (40 min) application of V3 agonist cocktail (50 μM 2-APB + 200 μM Carvacrol) dramatically increased TGase activity in primary cultured keratinocytes from WT but not V3 KO mice.

(I) V3 agonist cocktail induced an ~11-fold increase of TGase activity in WT keratinocytes.

Data in (E) and (I) are presented as the mean ± SEM. See also Figure S6.

Defective Epidermal Barrier Function and TGase Activity in TRPV3-Deficient Mice

In addition to hair abnormalities, the skin of newborn V3 KO and cKO mice was red in color (erythroderma), dry, and scaly (Figures 6A and 6B), resembling the skin phenotype of mice with defective barrier formation (Koch et al., 2000; Sevilla et al., 2007). Before hair penetration (P0–P3), the skin of V3 KO mice was rougher and shinier than that of WT. To measure skin barrier integrity, we used toluidine blue exclusion. In newborn (P0) V3 WT, KO, and E17 WT mice, dye was almost completely excluded, indicating normal maturation of the skin barrier. In E17 V3 KO embryos, however, dye permeability was significant, particularly in ventral areas (Figure 6C). EGF is known to increase the thickness of stratum corneum (Ponec et al., 1997), and consistent with a role for TRPV3 in barrier formation, the stratum corneum layer of V3 KO (Figure S2) and cKO (Figures 2C and 2D) mice was significantly thinner and more compact than WT littermates. We next examined the morphology of the mature CE. Mature CE in WT skin was symmetrical and smooth, whereas immature CE was irregular and fragile. The density of

Ca^{2+} is an important regulator of keratinocyte differentiation both in vitro and in vivo (Yuspa et al., 1989). We next examined Ca^{2+}-dependent keratinocyte differentiation in vitro using a well-established Ca^{2+} switch protocol. In these experiments, epidermal basal cells were selectively cultured in 0.05 mM Ca^{2+} medium and terminal differentiation was induced by raising $[Ca^{2+}]_o$ to 0.2–1.4 mM (Yuspa et al., 1989). Compared to WT cells, more loricrin was expressed in cultured V3 KO keratinocytes after induction of differentiation (Figure S5). Collectively, these results suggest a role of TRPV3 in keratinocyte differentiation both in vitro and in vivo.

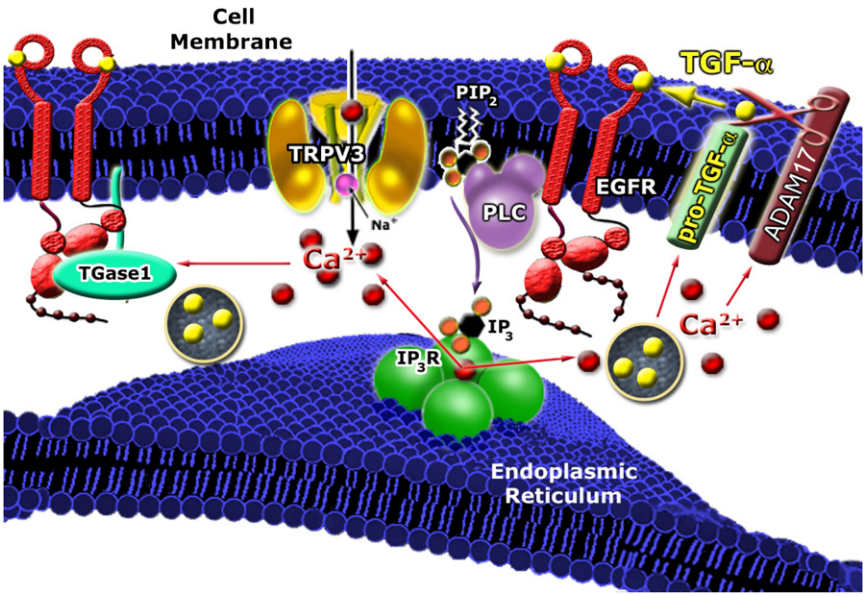

Figure 7. A Working Model for the Role of TRPV3 in Keratinocyte Cell Biology

Activation of TRPV3 in vivo (potentially by an endogenous mechanism such as temperature or other unidentified cellular cues) may lead to an increase of Ca^{2+}-dependent production/shedding/release of TGF-α or other EGFR ligands and an elevation of TGase (TGase1 and TGase3) activity. TGF-α in turn activates EGFR that physically associates with TRPV3 to form a signaling complex, which subsequently sensitizes TRPV3's responses to the putative endogenous activation mechanism(s). Thus, a positive-feedback loop is formed between TRPV3 and TGF-α/EGFR. The combined function(s) of the TRPV3/ADAM17/EGFR/TGase complex may lead to terminal differentiation of suprabasal keratinocytes. Impairment of TRPV3/EGFR signaling leads to a "wavy hair" phenotype. TRPV3/ADAM17/EGFR/TGases signaling is required for skin barrier formation; reduced activity leads to a "dry skin" phenotype. Dysregulation of the TRPV3/ADAM17/EGFR/TGase signaling axis might also lead to other skin diseases.

mature CE in V3 KO (Figure S6) and cKO mice (Figures 6D and 6E) was only 15%–18% of that in WT mice.

Multiple mechanisms might lead to defective CE formation. TGases are a family of enzymes that crosslink proteins essential for CE formation (Lorand and Graham, 2003). Among them, TGase1 and TGase3 are expressed in the epidermis and are regulated by intracellular Ca^{2+} (Lorand and Graham, 2003). One possibility is that the activity of TGases was reduced in V3 KO mice. EGF or TGF-α is known to dramatically increase the activity of TGases and CE formation in cultured keratinocytes in suspension, which presumably mimics the conditions of suprabasal keratinocytes (Wakita and Takigawa, 1999). We found that the activity of TGases (Koch et al., 2000; Raghunath et al., 1998) was significantly lower in both newborn (P1) and P4 V3 cKO epidermis (Figure 6F) but not in age-matched V1 and V4 KO epidermis (Figure S6). The expression level of TGase1, however, was comparable for WT and V3 cKO (Figure 6G). When TGase activity was measured in cultured keratinocytes, TGase activity was abnormally low in both WT and V3 KO keratinocytes (Figures 6H and 6I). Application of V3 agonist cocktail dramatically increased TGase activity (>10-fold) in WT but not V3 KO cells. Application of V1 and V4 agonists resulted in either no change or a slight increase in TGase activity in WT keratinocytes (Figure S6). These results suggest that activation of TRPV3 increased intracellular [Ca^{2+}], TGase activity, and subsequent CE formation in the epidermis.

DISCUSSION

Intracellular Ca^{2+} regulates both the production and the release of EGFR ligands (Denning et al., 2000; Dlugosz et al., 1994). As TGF-α production/release is an autoinduction process (Coffey et al., 1987), the reduced production of TGF-α might result from reduced EGFR activity. The positive feedback loop (Figure 7) in which TGF-α/EGFR activation potentiates TRPV3-mediated Ca^{2+} entry, which in turn potentiates TGF-α/EGFR signaling, may provide an explanation for its unique property of autoinduction (Coffey et al., 1987). Ca^{2+}-induced differentiation dramatically increases TGF-α production, suggesting a nonproliferative role of the TGF-α/EGFR signaling axis (Denning et al., 2000). On the other hand, EGF/TGF-α itself is known to promote late terminal differentiation both in vitro and in vivo by dramatically increasing TGase activity and CE formation while suppressing the expression of K10 (Dlugosz et al., 1994; Wakita and Takigawa, 1999). Thus, for suprabasal cells, the function of EGFR signaling is to promote late terminal differentiation (Wakita and Takigawa, 1999). The primary defect in V3 KO mice is late terminal differentiation but not proliferation. Thus, the feedforward mechanism described above may contribute to the process of late terminal differentiation.

It is still not clear how TRPV3 is activated to trigger or promote late terminal differentiation. Temperatures in the range of 31°C–39°C activate TRPV3 in heterologous expression systems (Ramsey et al., 2006). Thus temperature may be the primary activator for keratinocyte TRPV3. Consistent with this notion, temperature is known to affect the barrier function and modulate the effect of EGF/TGF-α on keratinocyte differentiation (Denda et al., 2007; Ponec et al., 1997). At skin temperatures in vivo (~32°C), TRPV3 is constitutively but weakly active. Thus release of TGF-α may increase the activity of weakly constitutively active TRPV3.

We provide evidence that TRPV3 and TGF-α/EGFR are in the same signaling complex regulating epidermal homeostasis. Whereas loss-of-function in TGF-α/EGFR leads to "wavy hair" (Luetteke et al., 1993, 1994; Mann et al., 1993; Schneider et al., 2008; Sibilia and Wagner, 1995; Threadgill et al., 1995), elevated TGF-α/EGFR activities cause a "hairless" phenotype (Ferby et al., 2006; Schneider et al., 2008; Wang et al., 2006). Interestingly, whereas our V3 KO mice exhibit "wavy hair," mice carrying a gain-of-function mutation in TRPV3 are hairless

(Asakawa et al., 2006). It may prove informative to generate transgenic mice with TRPV3 loss of function and concurrent TGF-α/EGFR gain of function, or with TRPV3 gain of function and concurrent TGF-α/EGFR loss of function.

EGFR is the prototype of the RTK family. EGFR signaling is necessary for proper development and tissue homeostasis whereas its dysregulation rapidly results in defects in cellular proliferation and differentiation. The consequences of its malfunction are abnormal hair follicle morphogenesis, impaired would healing, and tumorigenesis (Schneider et al., 2008). We have identified another key element in this important signaling pathway, the TRPV3 channel. Our studies not only provide the first in vivo evidence in mammals for the close interaction of RTK and TRP channels but also suggest that TRPV3 can be a novel target for hair growth and removal agents as well as in the treatment of skin cancers or other dermatological diseases.

EXPERIMENTAL PROCEDURES

Conditional and Global Disruption of *Trpv3* in Mice

Mouse *Trpv3* was disrupted either globally or in a keratinocytes-specific manner (see Extended Experimental Procedures in the Supplemental Information).

Real-Time Semiquantitative PCR

After a small piece of back skin was dissolved in TRIzol (Invitrogen, Carlsbad, CA, USA), mRNA was purified using RNeasy columns (QIAGEN Inc., Valencia, CA, USA). First-strand cDNA was synthesized using Superscript III RT (Invitrogen) and utilized for Semiquantitative PCR based on intron-spanning primers. A Bio-Rad iQ iCycler was used to measure the expression level of transcripts. The primer sequences are provided in the Extended Experimental Procedures.

Preparation and Culture of Mouse Keratinocytes

Mice (P0–P2) were sacrificed and soaked in 10% povidone-iodine for 5 min. After rinsing in 70% ethanol multiple times, the skin was removed and placed in a Petri dish containing PBS solution with 0.25% trypsin (Invitrogen) for incubating at 4°C overnight. Epidermis was then separated from the subcutaneous tissues. Vortexing dissociated cells and keratinocytes were first plated in a high $[Ca^{2+}]_o$ (1.4 mM) minimal essential medium (MEM; GIBCO), which was replaced with a low $[Ca^{2+}]_o$ (0.05 mM; differentiation-restricted) medium after 6 hr. The keratinocytes were then cultured in MEM containing 8% Chelex-treated (Bio-Rad) FBS with the final $[Ca^{2+}]$ adjusted to 0.05 mM. Suspension cultures were on polyhydroxyethylmethacrylate (poly-HEMA)-coated plates as described previously (Wakita and Takigawa, 1999).

NHEK Cell Culture

Normal human epidermal keratinocytes were obtained from Invitrogen and cultured in EpiLife Medium supplemented with Human Keratinocyte Growth Supplement (Invitrogen).

Immunoblotting and Immunoprecipitation

Back skin lysates for the immunodetection of EGFR and P-EGFR were prepared as follows: a small piece of back skin was lysed on ice for 30 min using 1 ml of lysis buffer (50 mM Tris [pH 7.4], 150 mM NaCl, 1 mM EDTA, 1% NP-40, 1 mM NaF, 1 mM Na_3VO_4, 1 mM PMSF, 0.25% sodium deoxycholate, and 1× protease inhibitor cocktail). Immuoprecipitation and immuoblotting were then performed using skin lysates as described in the Extended Experimental Procedures.

Histology and Immunostaining

Tissues were fixed for 3 hr with 4% paraformaldehyde (PFA) at 4°C, embedded in OCT or paraffin. Sections (~4 μm) of paraffin-embedded tissues were stained with hematoxylin and eosin (H&E). Immunohistochemistry was performed on cryostat sections (~10 μm) using antibody dilutions described in the Extended Experimental Procedures.

Dye Exclusion Assays

Toluidine blue staining of mouse embryos and newborn pups was performed as described in the Extended Experimental Procedures.

In Vivo and In Vitro Transglutaminase Activity Assay

Detection of TGase activity in skin sections (in vivo) and cultured keratinocytes (in vitro) used the amine donor substrate monodansylcadaverine (Molecular Probes) as described in the Extended Experimental Procedures.

Analysis of Cornified Envelopes

A piece of back skin (P4) was isolated and treated as described previously (Koch et al., 2000). Briefly, CEs were prepared by boiling skin for 30–60 min in a buffer consisting of 20 mM Tris-HCl, pH 7.5, 5 mM EDTA, 10 mM DTT, and 2% SDS. After centrifugation (5,000 *g*), CEs were washed twice at room temperature with a buffer consisting of 20 mM Tris-HCl, pH 7.5, 5 mM EDTA, 10 mM DTT, and 0.2% SDS. The density of CE was manually determined using a hemacytometer.

TGF-α ELISA

The medium of near confluent NHEK keratinocytes was harvested for TGF-α measurements using an ELISA kit for human TGF-α (Calbiochem).

Electrophysiology

Whole-cell recordings were performed in primary keratinocytes. Details of recording conditions are described in the Extended Experimental Procedures.

Ca^{2+} Imaging

Mouse and NHEK primary keratinocytes were loaded with 5 μM Fura-2 AM in culture medium at 37°C for 60 min. Cells were then washed in modified Tyrode's solution for 10–30 min. Fluorescence at different excitation wavelengths was recorded on an EasyRatioPro system (Photon Technology International, Birmingham, NJ, USA). Fura-2 ratios (F340/F380) recorded changes in $[Ca^{2+}]_i$ upon stimulation. Ionomycin (1 μM) was added at the conclusion of all experiments to induce a maximal response for comparison.

Data Analysis

Data are presented as the mean ± standard error of the mean (SEM). Statistical comparisons were made using analysis of variance (ANOVA). A p value < 0.05 was considered statistically significant.

SUPPLEMENTAL INFORMATION

Supplemental Information includes Extended Experimental Procedures and six figures and can be found with this article online at doi:10.1016/j.cell.2010.03.013.

ACKNOWLEDGMENTS

This work is supported by HHMI (to N.C.A and D.E.C), startup funds to H.X. from the Department of MCDB and Biological Science Scholar Program, and the University of Michigan and NIH RO1 grants (NS062792 to H.X. and AR045973 to A.A.D.). We thank Dr. Leonidas Tsiokas for the EGFR construct, Dr. Nan Hatch and Dr. Dave Ornitz for the FGFR2 constructs, and Dr. Makato Suzuki for TRPV4 KO mice. We are grateful to Y. Fujiwara (Division of Hematology Transgenic core facility), S. Hein, X. Wang (Rockefeller University), X. Wang, E. Mills, R. Hume, J. Kuwada, M. Akaaboune, and C. Collins for assistance and L. Yue and D. Ren for comments on an earlier version of the manuscript. We appreciate the encouragement and helpful comments from other members of the Xu and Clapham laboratories. D.E.C. is founder of Hydra, which is currently working on TRPV3 antagonists.

Received: August 27, 2009
Revised: December 28, 2009
Accepted: March 11, 2010
Published: April 15, 2010

REFERENCES

Asakawa, M., Yoshioka, T., Matsutani, T., Hikita, I., Suzuki, M., Oshima, I., Tsukahara, K., Arimura, A., Horikawa, T., Hirasawa, T., et al. (2006). Association of a mutation in TRPV3 with defective hair growth in rodents. J. Invest. Dermatol. *126*, 2664–2672.

Ballaro, C., Ceccarelli, S., Tiveron, C., Tatangelo, L., Salvatore, A.M., Segatto, O., and Alema, S. (2005). Targeted expression of RALT in mouse skin inhibits epidermal growth factor receptor signalling and generates a Waved-like phenotype. EMBO Rep. *6*, 755–761.

Byrne, C., Hardman, M., and Nield, K. (2003). Covering the limb–formation of the integument. J. Anat. *202*, 113–123.

Chung, M.K., Lee, H., Mizuno, A., Suzuki, M., and Caterina, M.J. (2004). TRPV3 and TRPV4 mediate warmth-evoked currents in primary mouse keratinocytes. J. Biol. Chem. *279*, 21569–21575.

Coffey, R.J., Jr., Derynck, R., Wilcox, J.N., Bringman, T.S., Goustin, A.S., Moses, H.L., and Pittelkow, M.R. (1987). Production and auto-induction of transforming growth factor-alpha in human keratinocytes. Nature *328*, 817–820.

Coulombe, P.A., Kopan, R., and Fuchs, E. (1989). Expression of keratin K14 in the epidermis and hair follicle: insights into complex programs of differentiation. J. Cell Biol. *109*, 2295–2312.

Denda, M., Sokabe, T., Fukumi-Tominaga, T., and Tominaga, M. (2007). Effects of skin surface temperature on epidermal permeability barrier homeostasis. J. Invest. Dermatol. *127*, 654–659.

Denning, M.F., Dlugosz, A.A., Cheng, C., Dempsey, P.J., Coffey, R.J., Jr., Threadgill, D.W., Magnuson, T., and Yuspa, S.H. (2000). Cross-talk between epidermal growth factor receptor and protein kinase C during calcium-induced differentiation of keratinocytes. Exp. Dermatol. *9*, 192–199.

Dlugosz, A.A., Cheng, C., Denning, M.F., Dempsey, P.J., Coffey, R.J., Jr., and Yuspa, S.H. (1994). Keratinocyte growth factor receptor ligands induce transforming growth factor alpha expression and activate the epidermal growth factor receptor signaling pathway in cultured epidermal keratinocytes. Cell Growth Differ. *5*, 1283–1292.

Du, X., Tabeta, K., Hoebe, K., Liu, H., Mann, N., Mudd, S., Crozat, K., Sovath, S., Gong, X., and Beutler, B. (2004). Velvet, a dominant Egfr mutation that causes wavy hair and defective eyelid development in mice. Genetics *166*, 331–340.

Ferby, I., Reschke, M., Kudlacek, O., Knyazev, P., Pante, G., Amann, K., Sommergruber, W., Kraut, N., Ullrich, A., Fassler, R., et al. (2006). Mig6 is a negative regulator of EGF receptor-mediated skin morphogenesis and tumor formation. Nat. Med. *12*, 568–573.

Fuchs, E., and Raghavan, S. (2002). Getting under the skin of epidermal morphogenesis. Nat. Rev. Genet. *3*, 199–209.

Horiuchi, K., Le Gall, S., Schulte, M., Yamaguchi, T., Reiss, K., Murphy, G., Toyama, Y., Hartmann, D., Saftig, P., and Blobel, C.P. (2007). Substrate selectivity of epidermal growth factor-receptor ligand sheddases and their regulation by phorbol esters and calcium influx. Mol. Biol. Cell *18*, 176–188.

Hu, H.Z., Gu, Q., Wang, C., Colton, C.K., Tang, J., Kinoshita-Kawada, M., Lee, L.Y., Wood, J.D., and Zhu, M.X. (2004). 2-aminoethoxydiphenyl borate is a common activator of TRPV1, TRPV2, and TRPV3. J. Biol. Chem. *279*, 35741–35748.

Huang, S.M., Lee, H., Chung, M.K., Park, U., Yu, Y.Y., Bradshaw, H.B., Coulombe, P.A., Walker, J.M., and Caterina, M.J. (2008). Overexpressed transient receptor potential vanilloid 3 ion channels in skin keratinocytes modulate pain sensitivity via prostaglandin E2. J. Neurosci. *28*, 13727–13737.

Koch, P.J., de Viragh, P.A., Scharer, E., Bundman, D., Longley, M.A., Bickenbach, J., Kawachi, Y., Suga, Y., Zhou, Z., Huber, M., et al. (2000). Lessons from loricrin-deficient mice: compensatory mechanisms maintaining skin barrier function in the absence of a major cornified envelope protein. J. Cell Biol. *151*, 389–400.

Li, H.S., Xu, X.Z., and Montell, C. (1999). Activation of a TRPC3-dependent cation current through the neurotrophin BDNF. Neuron *24*, 261–273.

Lorand, L., and Graham, R.M. (2003). Transglutaminases: crosslinking enzymes with pleiotropic functions. Nat. Rev. *4*, 140–156.

Luetteke, N.C., Qiu, T.H., Peiffer, R.L., Oliver, P., Smithies, O., and Lee, D.C. (1993). TGF alpha deficiency results in hair follicle and eye abnormalities in targeted and waved-1 mice. Cell *73*, 263–278.

Luetteke, N.C., Phillips, H.K., Qiu, T.H., Copeland, N.G., Earp, H.S., Jenkins, N.A., and Lee, D.C. (1994). The mouse waved-2 phenotype results from a point mutation in the EGF receptor tyrosine kinase. Genes Dev. *8*, 399–413.

Mann, G.B., Fowler, K.J., Gabriel, A., Nice, E.C., Williams, R.L., and Dunn, A.R. (1993). Mice with a null mutation of the TGF alpha gene have abnormal skin architecture, wavy hair, and curly whiskers and often develop corneal inflammation. Cell *73*, 249–261.

Miettinen, P.J., Berger, J.E., Meneses, J., Phung, Y., Pedersen, R.A., Werb, Z., and Derynck, R. (1995). Epithelial immaturity and multiorgan failure in mice lacking epidermal growth factor receptor. Nature *376*, 337–341.

Montell, C. (2005). The TRP superfamily of cation channels. Sci. STKE *2005*, re3.

Moqrich, A., Hwang, S.W., Earley, T.J., Petrus, M.J., Murray, A.N., Spencer, K.S., Andahazy, M., Story, G.M., and Patapoutian, A. (2005). Impaired thermosensation in mice lacking TRPV3, a heat and camphor sensor in the skin. Science *307*, 1468–1472.

Murillas, R., Larcher, F., Conti, C.J., Santos, M., Ullrich, A., and Jorcano, J.L. (1995). Expression of a dominant negative mutant of epidermal growth factor receptor in the epidermis of transgenic mice elicits striking alterations in hair follicle development and skin structure. EMBO J. *14*, 5216–5223.

Nilius, B., Owsianik, G., Voets, T., and Peters, J.A. (2007). Transient receptor potential cation channels in disease. Physiol. Rev. *87*, 165–217.

Pandiella, A., and Massague, J. (1991). Multiple signals activate cleavage of the membrane transforming growth factor-alpha precursor. J. Biol. Chem. *266*, 5769–5773.

Peier, A.M., Reeve, A.J., Andersson, D.A., Moqrich, A., Earley, T.J., Hergarden, A.C., Story, G.M., Colley, S., Hogenesch, J.B., McIntyre, P., et al. (2002). A heat-sensitive TRP channel expressed in keratinocytes. Science *296*, 2046–2049.

Peschon, J.J., Slack, J.L., Reddy, P., Stocking, K.L., Sunnarborg, S.W., Lee, D.C., Russell, W.E., Castner, B.J., Johnson, R.S., Fitzner, J.N., et al. (1998). An essential role for ectodomain shedding in mammalian development. Science *282*, 1281–1284.

Peus, D., Hamacher, L., and Pittelkow, M.R. (1997). EGF-receptor tyrosine kinase inhibition induces keratinocyte growth arrest and terminal differentiation. J. Invest. Dermatol. *109*, 751–756.

Ponec, M., Gibbs, S., Weerheim, A., Kempenaar, J., Mulder, A., and Mommaas, A.M. (1997). Epidermal growth factor and temperature regulate keratinocyte differentiation. Arch. Dermatol. Res. *289*, 317–326.

Raghunath, M., Hennies, H.C., Velten, F., Wiebe, V., Steinert, P.M., Reis, A., and Traupe, H. (1998). A novel in situ method for the detection of deficient transglutaminase activity in the skin. Arch. Dermatol. Res. *290*, 621–627.

Ramsey, I.S., Delling, M., and Clapham, D.E. (2006). An introduction to TRP channels. Annu. Rev. Physiol. *68*, 619–647.

Sakai, Y., Nelson, K.G., Snedeker, S., Bossert, N.L., Walker, M.P., McLachlan, J., and DiAugustine, R.P. (1994). Expression of epidermal growth factor in suprabasal cells of stratified squamous epithelia: implications for a role in differentiation. Cell Growth Differ. *5*, 527–535.

Schneider, M.R., Werner, S., Paus, R., and Wolf, E. (2008). Beyond wavy hairs: the epidermal growth factor receptor and its ligands in skin biology and pathology. Am. J. Pathol. *173*, 14–24.

Sevilla, L.M., Nachat, R., Groot, K.R., Klement, J.F., Uitto, J., Djian, P., Maatta, A., and Watt, F.M. (2007). Mice deficient in involucrin, envoplakin, and periplakin have a defective epidermal barrier. J. Cell Biol. *179*, 1599–1612.

Sibilia, M., and Wagner, E.F. (1995). Strain-dependent epithelial defects in mice lacking the EGF receptor. Science *269*, 234–238.

Threadgill, D.W., Dlugosz, A.A., Hansen, L.A., Tennenbaum, T., Lichti, U., Yee, D., LaMantia, C., Mourton, T., Herrup, K., Harris, R.C., et al. (1995). Targeted disruption of mouse EGF receptor: effect of genetic background on mutant phenotype. Science *269*, 230–234.

Wakita, H., and Takigawa, M. (1999). Activation of epidermal growth factor receptor promotes late terminal differentiation of cell-matrix interaction-disrupted keratinocytes. J. Biol. Chem. *274*, 37285–37291.

Wang, X., Zinkel, S., Polonsky, K., and Fuchs, E. (1997). Transgenic studies with a keratin promoter-driven growth hormone transgene: prospects for gene therapy. Proc. Natl. Acad. Sci. USA *94*, 219–226.

Wang, X., Bolotin, D., Chu, D.H., Polak, L., Williams, T., and Fuchs, E. (2006). AP-2alpha: a regulator of EGF receptor signaling and proliferation in skin epidermis. J. Cell Biol. *172*, 409–421.

Watanabe, H., Davis, J.B., Smart, D., Jerman, J.C., Smith, G.D., Hayes, P., Vriens, J., Cairns, W., Wissenbach, U., Prenen, J., et al. (2002). Activation of TRPV4 channels (hVRL-2/mTRP12) by phorbol derivatives. J. Biol. Chem. *277*, 13569–13577.

Xu, H., Ramsey, I.S., Kotecha, S.A., Moran, M.M., Chong, J.A., Lawson, D., Ge, P., Lilly, J., Silos-Santiago, I., Xie, Y., et al. (2002). TRPV3 is a calcium-permeable temperature-sensitive cation channel. Nature *418*, 181–186.

Xu, H., Delling, M., Jun, J.C., and Clapham, D.E. (2006). Oregano, thyme and clove-derived flavors and skin sensitizers activate specific TRP channels. Nat. Neurosci. *9*, 628–635.

Yuspa, S.H., Kilkenny, A.E., Steinert, P.M., and Roop, D.R. (1989). Expression of murine epidermal differentiation markers is tightly regulated by restricted extracellular calcium concentrations in vitro. J. Cell Biol. *109*, 1207–1217.

EXTENDED EXPERIMENTAL PROCEDURES

Conditional and Global Disruption of Trpv3 in Mice

We targeted exon 13 of mouse *Trpv3*, located on chromosome 11 B4, to disrupt its function. Deletion of exon 13 was predicted to remove the entire 3rd transmembrane segment (TM3) and part of TM4 and shift the open reading frame thereafter (see Figure S1). Thus, the putative pore region (TM5-TM6) would not be translated in TRPV3 KO mice regardless of whether the resulting transcript was stable. Since global knockout mice can be easily obtained from conditional deletions via a global Cre transgenic, such as *Sox2-Cre* (Hayashi et al., 2002), we made a construct for conditional disruption of *Trpv3* based on a recombineering method (Liu et al., 2003). In this construct, exon 13 of *Trpv3* was flanked by two LoxP sites plus an FRT-flanked neomycin resistance cassette (see Figure S1). This modified allele is referred to as $Trpv3^{flneo}$. Deletion of the FRT-flanked neomycin resistance cassette via the recombinase results in the floxed allele referred to as $Trpv3^{fl}$. Deletion of the floxed exon 13 results in a null allele, referred to as $Trpv3^{-}$. For ES cell targeting, the construct was electroporated into J1 embryonic stem cells and cells were selected for neomycin resistance. Positive ES cell clones with correct homologous recombination were identified by Southern analysis. Three positive ES cell clones with a normal karyotype were injected into C57BL/6J mouse blastocysts and transferred into the uteri of pseudopregnant females, from which three high-percentage male chimeras were obtained. The chimeras were bred with C57BL/6J females to generate F1 offspring carrying the $Trpv3^{flneo}$ allele. Germline transmission of the $Trpv3^{flneo}$ allele was confirmed by Southern analysis using tail DNA prepared from Agouti pups. The neomycin resistance cassette was removed from the targeted allele by breeding $Trpv3^{flneo/+}$ mice with transgenic mice expressing the Flp recombinase (Farley et al., 2000) (Jackson Laboratory #003946), resulting in $Trpv3^{fl/+}$ mice. The $Trpv3^{-/+}$ mice were obtained by breeding $Trpv3^{fl/+}$ mice with *Sox-2-Cre* transgenic which provides germline/embryonic expression of Cre recombinase (Hayashi et al., 2002). $Trpv3^{fl/fl}$ and $Trpv3^{-/-}$ mice were obtained, respectively, by intercross of heterozygotes and maintained on a mixed C57BL/6J and 129/SvEvTac background. $Trpv3^{-/-}$ mice were also backcrossed with C57BL/6J females for more than 6 generations to obtain a clean genetic background. K14-Cre transgenic (Jackson laboratory # 004782) was bred with $Trpv3^{fl/fl}$ mice to obtain keratinocyte-specific disruption of *Trpv3*.

Southern Blot and PCR Genotyping

For Southern blot analysis, 10 μg of genomic DNA was digested overnight with KpnI, fractionated on a 0.7% agarose gel, and transferred to Hybond N+ membrane (Amersham). Southern analysis was performed using a standard non-radioactive labeling protocol with DIG-labeled dTTP (Roche). The probe for identification of the $Trpv3^{flneo}$ allele generated by homologous recombination was amplified with the following primers: 5′- CAATGAAAAGAGTCTACAGCTTTGGA-3′ and 5′ CTACATGGGGCAGTTCCAAGATC-3′. Mouse genotyping was routinely done by PCR analysis. For $Trpv3^{fl/+}$ mice, F8305, 5′- GCTGGTTGGGCATTGGTAAGAG-3′, and R8432, 5′- GTCTGTTATATGTACAGGCATGG-3′ were used (Primer set B). The $Trpv3^{fl}$ and wt alleles yielded products of 200 bp and 130 bp, respectively. For $Trpv3^{-/+}$ mice, F7656, 5′- GACATGCCATGCAAAAAACTACCA-3′ and R8432 (Primer set A) were used: the null and alleles yielded products of 300 bp and 800 bp, respectively. The primers for Cre are as follows:

forward primer (F), 5′- CGTATAGCCGAAATTGCCAG-3′;

reverse primer (R), 5′- CAAAACAGGTAGTTATTCGG-3′

Genotypes of TRPV4 KO mice and K14 promoter- driven TRPV3-YFP transgenic mice were determined by PCR as described previously (Huang et al., 2008; Suzuki et al., 2003).

Real-Time Semiquantitative PCR

The primer sequences were as follows.

For mL32, F: 5′-TGGTGAAGCCCAAGATCGTC-3′; R: 5′- CTTCTCCGCACCCTGTTGTC-3′.

For mTGF-α, F: 5′- GCGCTGGGTATCCTGTTAGC-3′; R: 5′-TGGGAATCTGGGCACTTGTT-3′.

h EGFR F: 5′-CGGGACATAGTCAGCAGTGA-3′; R: 5′-GGGACAGCTTGGATCACACT-3′

h PLC-γ1 F: 5′-TGGCTCCGGAAGCAGTTTTA-3′; R: 5′-ATGTTGGGGACCCGGTAGTT-3′

h GADPH F: 5′-GAAGGTGAAGGTCGGAGTCA-3′; R: 5′- AATGAAGGGGTCATTGATGG-3′

m EGF F: 5′-GGTGGCTCCGTCCGTCTTAT-3′; R: 5′-CCAAATCGCCTTGCTTTTCA-3′

m AR F: 5′-CATCGGCATCGTTATCACAG-3′; R: 5′-ACAGTCCCGTTTTCTTGTCG-3′

m HBEGF F: 5′-ATCCACGGGGAGTGCAGATA-3′; R: 5′-GAGTCAGCCCATGACACCTG-3′

m EGFR F: 5′-CGGGACACCCAATCAGAAAA-3′; R: 5′-CAGCCTTCCGAGGAGCATAA-3′

For each sample, the expression levels of mTGF-α, mEGF, mAR, mHBEGF, and mEGFR were normalized using that of mL32. The expression levels of hEGFR and hPLC-γ1were normalized using that of hGADPH.

Reverse Transcriptional-PCR Analysis

Single-stranded cDNA from P0 mouse skin was prepared as described in Experimental Procedures. Primer sequences of TRPV3 were as follows.

Primer set C: forward primer, 5′- CAGCGTCATGATCCAGAAGG-3′; reverse primer 5′- ATCAGTGAGGCCAGCGCTAC-3′.

Primer set D: forward primer, 5′- TGCTGAGACCCTCCGATCTT-3′; reverse primer, 5′- GGCAGGCGAGGTATTCTTTG-3′.

Primer set D was designed based on sequences within the putative deletion region, exon 13.

Lentiviral pLKO.1-ShRNA Knockdown

A series of Lentiviral pLKO.1-ShRNA constructs against human EGFR and PLC-γ1 were purchased from Sigma and tested using q-PCR in HEK293T cells. The following two ShRNA constructs were chosen to knock down EGFR and PLC-γ1 in human epidermal keratinocytes (NHEK):

EGFR: 5′-CCGGGCTGCTCTGAAATCTCCTTTACTCGAGTAAAGGAGATTTCAGAGCAGCTTTTTG-3′;

PLC-γ1: 5′-CCGGCCAGATCAGTAACCCTGAATTCTCGAGAATTCAGGGTTACTGATCTGGTTTTT-3′.

The ShRNA and pLKO.1 control lentivirus stocks were generated via co-transfection of HEK293T cells with packaging plasmids VSV-G-pMAD.G and pCMVdeltaR8.91. NHEK cells were infected with each lentivirus stock and 3 days post-puromycin (2 μg/ml) selection, were used for Ca^{2+} imaging experiments.

Immunoblotting and Immunoprecipitation

For the immunodetection of EGFR and P-EGFR, back skin lysates were incubated with 2 μg of EGFR antibody (Upstate Cell Signaling) and rotated for 12 hr at 4°C. Protein A/G beads (30 μl; Amersham Pharmacia) were added, and after 12 hr incubation, the beads were pulled down and washed 5–6 times with lysis buffer. Bound proteins were eluted from the beads with SDS (1×) sample buffer, vortexed, boiled for 5 min, and analyzed by immunoblotting. The total cell lysate or immunoprecipitated proteins were separated by SDS-PAGE and transferred to nitrocellulose membranes. The membranes were blocked for 1 hr with 5% skim milk in PBST and incubated with the anti-EGFR or P-EGFR antibody (diluted 1:1000) in PBST. Detection was carried out using Peroxidase-conjugated anti-rabbit secondary antibody with an enhanced chemiluminescence reagent (Amersham Pharmacia Biotech).

Co-immunoprecipitation for TRPV3 and EGFR was performed in skin lysates or HEK293T cells transfected with pEGFP-C3, TRPV3-EGFP, and EGFR plasmids. The lysis buffer contained 137 mM NaCl, 10% glycerol, 1% NP-40, 2 mM EDTA, and 20 mM Tris-HCl (pH 8.0). The lysate was stirred on ice for 30 min and then centrifuged. The supernatant was incubated with anti-EGFR (Upstate) or anti-GFP (Covance) at 4°C overnight. The protein complex was then visualized by western blotting using antibodies against GFP or EGFR (Upstate).

Histology and Immunostaining

Immunohistochemistry was performed on cryostat sections (~10 μm) using antibodies for K14 (1:5000; Covance), K1 (1:2000; Covance), K10 (1:1000; Sigma), Integrin α6 (1:1000; BD Lab), Integrin β4 (1:1000; BD Lab), Loricrin, (1:5000; Abcam), EGFR (1:200; Upstate Biotechnology), and P-EGFR (anti-P-Tyr 1173 EGFR, 1:200; Upstate Biotechnology). Nuclei were counterstained with DAPI reagents. Images were taken using an Olympus (IX 81) microscope and a Leica (TCS SP5) confocal microscope.

Dye Exclusion Assays

Toluidine blue staining of mouse embryos and newborn pups was preformed as described previously (Koch et al., 2000; Sevilla et al., 2007). The developmental stage of mouse embryos was determined based on the assumption that fertilization occurred in the middle of the day's dark cycle before vaginal plugs were identified. Embryos were dehydrated by incubation in 25%, 50%, and 75% methanol/PBS for 1 min each followed by incubation in 100% methanol for 1 min. The embryos were then rehydrated with the same series of methanol solution for 1 min each, washed in PBS, and stained for 10 min in 0.0125% toluidine blue O (Fisher Scientific)/PBS. The embryos were then de-stained in PBS.

In Vivo Transglutaminase Activity Assay

Detection of TGase activity in skin sections (Raghunath et al., 1998) used the amine donor substrate monodansylcadaverine (Molecular Probes). A solution of 2 mg biotinylated-X-cadaverine in 0.1 N HCl (50 μl) was prepared and then mixed with 394 μl doubly distilled H_2O. This 10 mM stock solution was stored at −20°C before use. TGases substrate buffer was prepared by adding 10 μl of the substrate stock solution plus 25 μl $CaCl_2$ (200 mM) solution to 965 μl Tris/HCl (100 mM; pH 8.4). Cryostat sections (~10 μm) were air-dried and preincubated with 1× BSA in 0.1 M Tris/HCl (pH 8.4) for 30 min at room temperature. The sections were then incubated for 2 hr with the substrate buffer (pH 8.4). The TGase reaction was stopped with PBS/25 mM EDTA (5 min) and washed two times with 1× PBS, 10 min each. The sections were incubated with Streptavidin-conjugated Alexa Fluor 488 (1:1000, Invitrogen) in PBS for 30 min, washed three times in PBS, and mounted for visualization.

In Vitro Transglutaminase Activity Assay (for Cultured Keratinocytes)

TGase activity in cultured keratinocytes was detected using the amine donor substrate monodansylcadaverine. Primary cultured keratinocytes were partially serum-starved overnight (1% FBS) in MEM medium containing 0. 5 mM Ca^{2+} medium. The cells were then treated with 0.1% DMSO, TRPV3 agonist cocktail (50 μM 2-APB + 200 μM Carvacrol) in MEM medium containing 1.4 mM Ca^{2+} and 100 μM biotinylated-X-cadaverine (Invitrogen) for 40 min. Keratinocytes were then rinsed in PBS, fixed with 4% PFA, and incubated with streptavidin-conjugated Alexa Fluor 488 (1:1000, Invitrogen) for 1 hr. Nuclei were counterstained with DAPI reagents for 10 min before microscopic observation.

TGF-α ELISA

To measure TGF-α release, near confluent NHEK keratinocytes were pretreated with or without the metalloproteinase inhibitor BB-2116 (20 μM; British Biotechnology, Oxford, UK) in the presence of 100 ng/ml EGF or 1 mM Tyrphostin AG 1478 (an EGFR inhibitor; Cell Signaling), which was expected to block EGFR activation and receptor-mediated endocytosis of TGF-α. Cells were then treated with V3 agonist cocktail (100 μM 2-APB + 250 μM Carvacrol) or 1 μM PMA (Cell Signaling) for 30 min in the presence or absence of 20 μM BB-2116. The medium was then harvested for TGF-α measurements using an ELISA kit for human TGF-α (Calbiochem).

Electrophysiology

Whole-cell patch-clamp recordings were performed in primary keratinocytes. The pipette solution contained 147 mM Cs, 120 mM methane-sulfonate, 4 mM NaCl, 10 mM EGTA, 2 mM Na_2-ATP, 2 mM $MgCl_2$, 20 mM HEPES (pH 7.2; free $[Ca^{2+}]_i < 10$ nM). Standard extracellular bath solution (modified Tyrode's solution) contained 153 mM NaCl, 5 mM KCl, 2 mM $CaCl_2$, 1 mM $MgCl_2$, 20 mM HEPES, 10 mM glucose (pH 7.4). All solutions were applied via a perfusion system to achieve a complete solution exchange within a few seconds. Data were collected using an Axopatch 2A patch clamp amplifier, Digidata 1440, and pClamp 10.0 software (Axon Instruments). Whole-cell currents were digitized at 10 kHz and low pass filtered at 2 kHz. Capacity current was reduced as much as possible using the amplifier circuitry; series resistance compensation was 60%–85%. For heat activation experiments, the perfusate was heated using a Warner TC-325B temperature controller and an SH-27B solution heater as described previously (Xu et al., 2006). All other experiments were conducted at room temperature (~21°C–23°C). All recordings were analyzed with pCLAMP10 (Axon Instruments, Union City, CA, USA) and Origin 7.5 (OriginLab, Northampton, MA, USA).

SUPPLEMENTAL REFERENCES

Farley, F.W., Soriano, P., Steffen, L.S., and Dymecki, S.M. (2000). Widespread recombinase expression using FLPeR (flipper) mice. Genesis *28*, 106–110.

Hayashi, S., Lewis, P., Pevny, L., and McMahon, A.P. (2002). Efficient gene modulation in mouse epiblast using a Sox2Cre transgenic mouse strain. Mech. Dev. *119* (*Suppl 1*), S97–S101.

Liu, P., Jenkins, N.A., and Copeland, N.G. (2003). A highly efficient recombineering-based method for generating conditional knockout mutations. Genome Res. *13*, 476–484.

Suzuki, M., Mizuno, A., Kodaira, K., and Imai, M. (2003). Impaired pressure sensation in mice lacking TRPV4. J. Biol. Chem. *278*, 22664–22668.

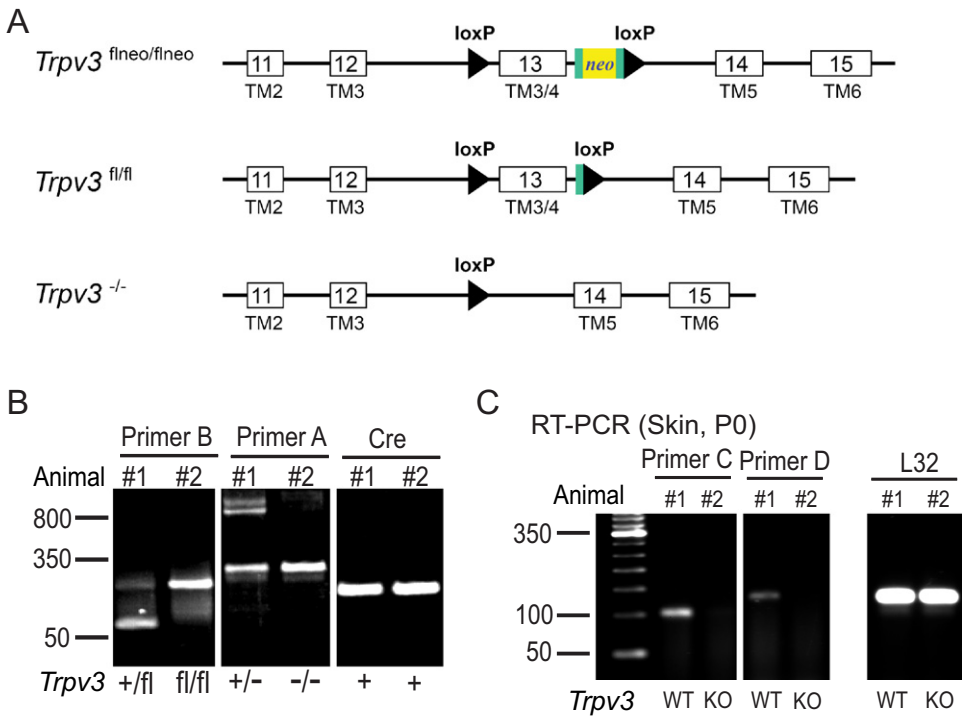

Figure S1. Generation of TRPV3-Deficicient Mice, Related to Figure 1

(A) Mouse *Trpv3* gene targeting strategy. A construct was designed for conditional disruption of *Trpv3* based on a recombineering method (see Experimental Procedures). In this construct, exon 13 of *Trpv3* was flanked by two LoxP sites plus an FRT-flanked neomycin resistance cassette. This modified allele is referred to as $Trpv3^{flneo}$. Deletion of the FRT-flanked neomycin resistance cassette via the Flp recombinase results in the floxed allele referred to as $Trpv3^{fl}$. Deletion of the floxed exon 13 results in a null allele, referred to as $Trpv3^{-}$.

(B) Keratinocyte-specific targeted deletion of *Trpv3*. PCR genotyping of TRPV3 K14-Cre conditional KO mice. Primers for genotyping and Cre transgene are described in Extended Experimental Procedures. PCR products for primer set B: fl allele 200 bp; WT 130 bp; Primer set A: WT 800 bp, null allele 300 bp; Cre: 200 bp.

(C) Absence of TRPV3 mRNA expression in the skin of V3 KO mice. TRPV3 mRNA was detected by RT-PCR method using two pairs of primers. Primer set D was designed to span the region to be deleted. The expression level of ribosomal protein L32, a housekeeping gene, served as a loading control.

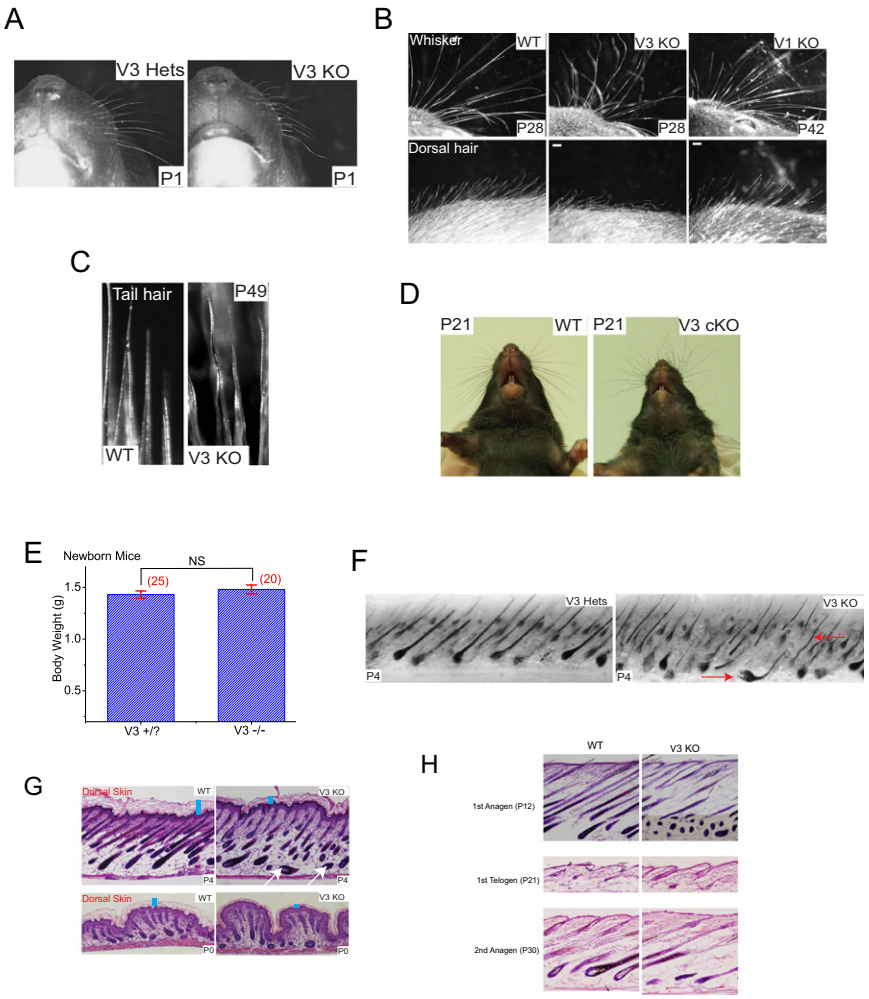

Figure S2. TRPV3-Deficinet Mice Exhibit Curly Whiskers, Wavy Hair, and Misaligned Hair Follicles, Related to Figure 2

(A) Whisker abnormality of newborn TRPV3 global KO mice. Whiskers (vibrissae) of newborn (P1) heterozygous mice were straight; the whiskers of littermate V3 KO mice were visibly kinked.

(B) TRPV3 KO, but not WT or TRPV1 KO mice, exhibited curly whiskers and wavy dorsal coats. Whiskers in an adult WT mouse (P28) were straight; the whiskers of littermate V3 KO mice were distinctively curly and hooked (upper panels). In contrast, the whiskers of TRPV1 KO mice (P42) were straight. Similarly, V3 KO, but not WT or TRPV1 KO mice, exhibited wavy dorsal coats (lower panels).

(C) "Wavy" tail hair of adult V3 KO mice.

(D) Wavy hair phenotype of V3-deficient mice is independent of genetic background and pigmentation. V3 cKO mice in a genetic background of black pigmentation (C57BL/6) exhibited curly whiskers and wavy hair (ventral view).

(E) Comparable body weight for newborn V3 KO and control mice. V3 KO ($V3^{-/-}$) and control ($V3^{+/?}$; $V3^{+/-}$, or $V3^{+/+}$) mice were determined based on whisker morphology and/or PCR genotyping.

(F) Hair follicle abnormality of TRPV3-deficient mice. Misaligned and curved hair follicles (arrow) in the intact skin from V3 KO mice (P4). Littermate heterozygotes served as controls.

(G) Skin and hair follicle abnormalities of V3-deficient mice revealed by H&E staining of dorsal skin sections from WT and V3 KO mice. (Upper panels) H&E stained sections (dorsal skin) from V3 KO mice. Arrows indicated two curved hair follicles of V3 KO mice. Note the thin stratum corneum. Thin and compact stratum corneum was observed in the dorsal (upper panels) and tail (lower panels) skins of neonatal (P0) V3 KO mice.

(H) Normal hair cycle of V3-deficient mice revealed by H&E staining of dorsal skin sections from WT and V3 KO mice.

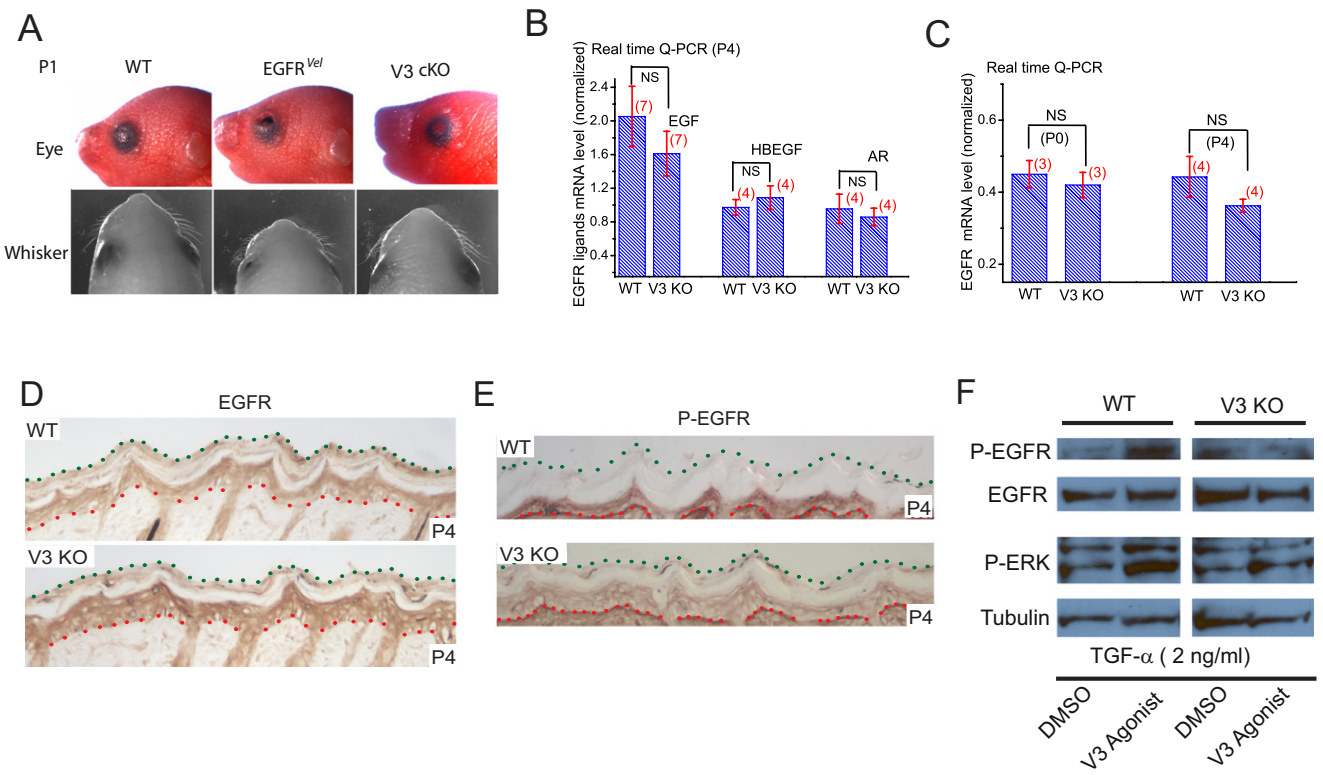

Figure S3. Decreased Activity of EGFR in the Skin of TRPV3-Deficient Mice, Related to Figure 3

(A) TRPV3-deficient mice exhibit curly whiskers, but not open eyelids at birth. Neonatal (P0) antimorphic EGFR^{Vel} mice were born with eyelids open, whereas the eyelids of WT mice or V3 cKO mice remained closed until several days after birth (upper panels). Both EGFR^{Vel} and V3 cKO mice exhibited curly whiskers (lower panels).

(B) Normal expression levels of EGF, HB-EGF, and AR in the skin of TRPV3-deficient mice. mRNA expression levels (q-PCR) of EGF, HB-EGF, and AR in the V3 KO skin tissues (P4) were not significantly ($p > 0.05$) different from WT skin.

(C) Normal mRNA expression level of EGFR in the skin of TRPV3-deficient mice. At P0 or P4, mRNA expression levels (q-PCR) of EGFR in the V3 KO skin tissues were not significantly ($p > 0.05$) different from WT skin.

(D and E) Reduced EGFR activity in the epidermis of TRPV3-deficient mice. Immunohistochemical staining of frozen skin sections from WT and V3 KO pups (P4). (D) Compared to WT mice, total EGFR staining appeared to be more intense in skin sections from V3 KO mice. (E) In contrast, P-EGFR immunostaining was more prominent in the basal layer of WT skin sections, although weak P-EGFR staining was detected in both basal and suprabasal layers of V3 KO skin sections. Red dotted lines denote dermo-epidermal borders; green dotted lines denote the surface of the epidermis.

(F) Activation of TRPV3 increases the response of EGFR to low concentrations of TGF-α in mouse keratinocytes. TGF-α-induced EGFR activity was measured with P-EGFR immunoreactivity. Wild-type and V3 KO keratinocytes were treated with TGF-α (2 ng/ml) in the presence and absence of V3 agonist cocktail (100 μM 2-APB + 250 μM Carvacrol) for 30 min.

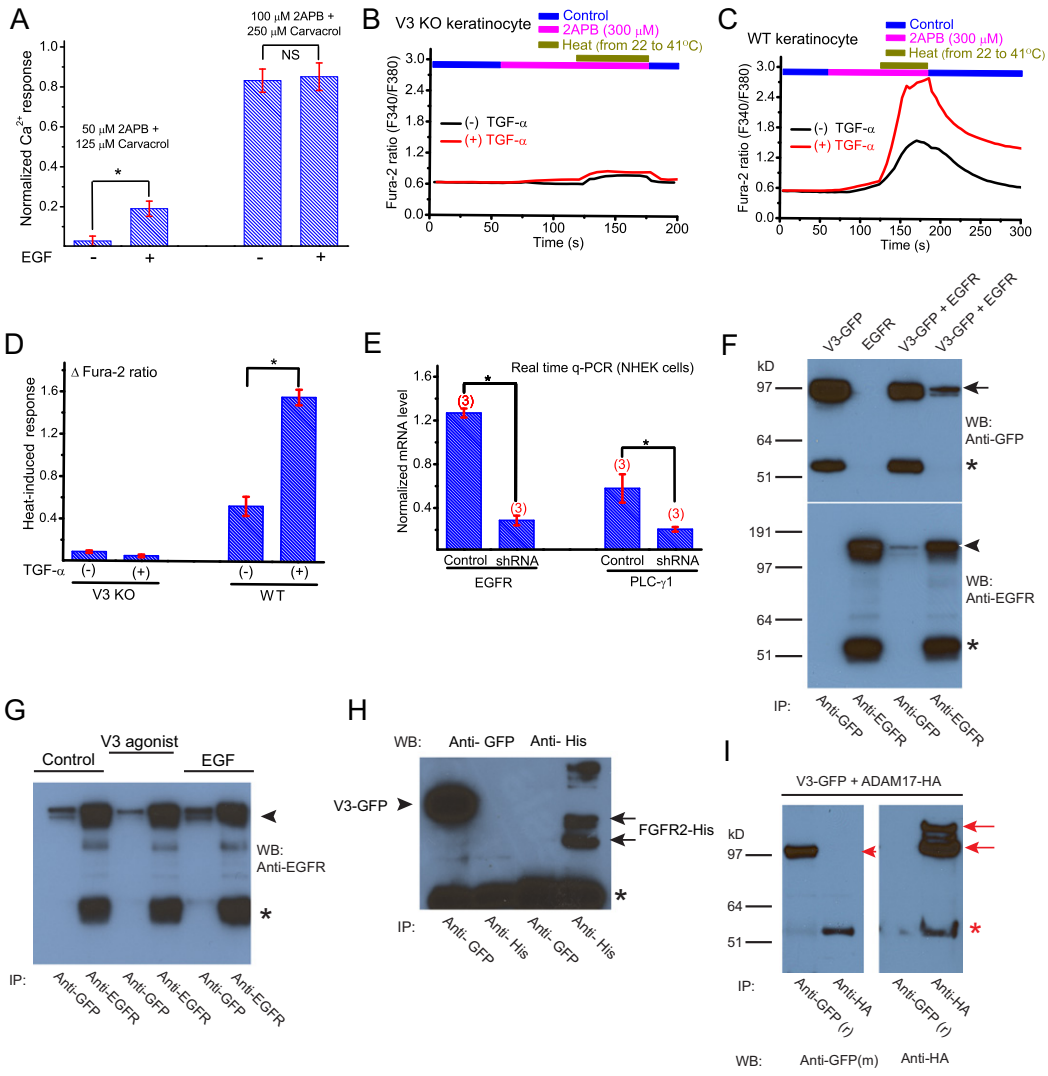

Figure S4. EGFR Associates with TRPV3 and Mediates PLC-Dependent Sensitization of TRPV3 Channel Activity in the Keratinocytes, Related to Figure 4

(A) Sensitizing effect of EGF in mouse primary keratinocytes. The effect of EGF (100 ng/ml) on V3 Ca^{2+} responses in mouse keratinocytes.

(B–D) TGF-α sensitizes the heat-induced Ca^{2+} responses of mouse keratinocytes. (B) Increase of bath temperature from 22°C to 41°C failed to induce significant Ca^{2+} increases in V3 KO keratinocytes, treated with or without TGF-α (100 ng/ml). Temperature-induced responses were measured in the presence of 300 μM 2-APB. (C) TGF-α treatment increased the responses of WT keratinocytes to changes in temperature. (D) Average sensitizing effect of TGF-α to the temperature-induced responses of WT keratinocytes.

(E) ShRNA-mediated knockdown of EGFR and PLC-γ1 in primary human keratinocytes. mRNA expression levels (q-PCR) of EGFR and PLC-γ1 were significantly reduced by shRNA treatment of NHEK cells.

(F) Coimmunopreciptation of TRPV3 and EGFR from HEK293 heterologous expression. HEK293 cells were transiently transfected with the cDNAs indicated (top). Immunoprecipitates (IP) were formed with the indicated antibodies and visualized on western blot. TRPV3-GFP was IP/WB'd by a monoclonal anti-GFP; TRPV3-GFP band indicated by arrowhead. EGFR was IP/WB'd by polyclonal anti-EGFR; EGFR band indicated by arrow. Heavy chain bands (~55 kDa) indicated by asterisks.

(G) Coimmunopreciptation of TRPV3 and EGFR is not dependent on activation of TRPV3 or EGFR. HEK293 cells were transiently transfected with both V3-GFP and EGFR expression constructs. Cells were treated with V3 agonist cocktail (100 μM 2-APB + 250 μM Carvacrol) or EGF (100 ng/ml) for 30 min. Immunoprecipitates (IP) were formed with the indicated antibodies and visualized on western blot. TRPV3-GFP was IP'd by a monoclonal anti-GFP antibody. EGFR was IP/WB'd by polyclonal anti-EGFR; EGFR band indicated by arrowhead. Heavy chain bands (~55 kDa) indicated by asterisks.

(H) TRPV3 does not immunoprecipitate FGFR2 in HEK293 heterologous expression system. HEK293 cells were transiently transfected with the cDNAs of V3-GFP and FGFR2-His. TRPV3-GFP was IP/WB'd by a monoclonal anti-GFP antibody; TRPV3-GFP band indicated by arrowhead. FGFR2 was IP/WB'd by an anti-His antibody; FGFR2 band indicated by arrow. Heavy chain bands (~55 kDa) indicated by asterisks.

(I) TRPV3 does not coimmunoprecipitate with ADAM17. HEK293 cells stably expressing ADAM17-HA were transiently transfected with TRPV3-EGFP cDNA. Immunoprecipitates (IP) were formed with the indicated antibodies and visualized on western blot. TRPV3-GFP was IP'd by a polyclonal anti-GFP(r) and WB'd by a monoclonal Anti-GFP antibody (m); TRPV3-GFP band indicated by arrowhead. ADAM17 was IP/WB by anti-HA antibody (m); ADAM17-HA band indicated by arrows. Heavy chain bands (~55 kDa) indicated by asterisks.

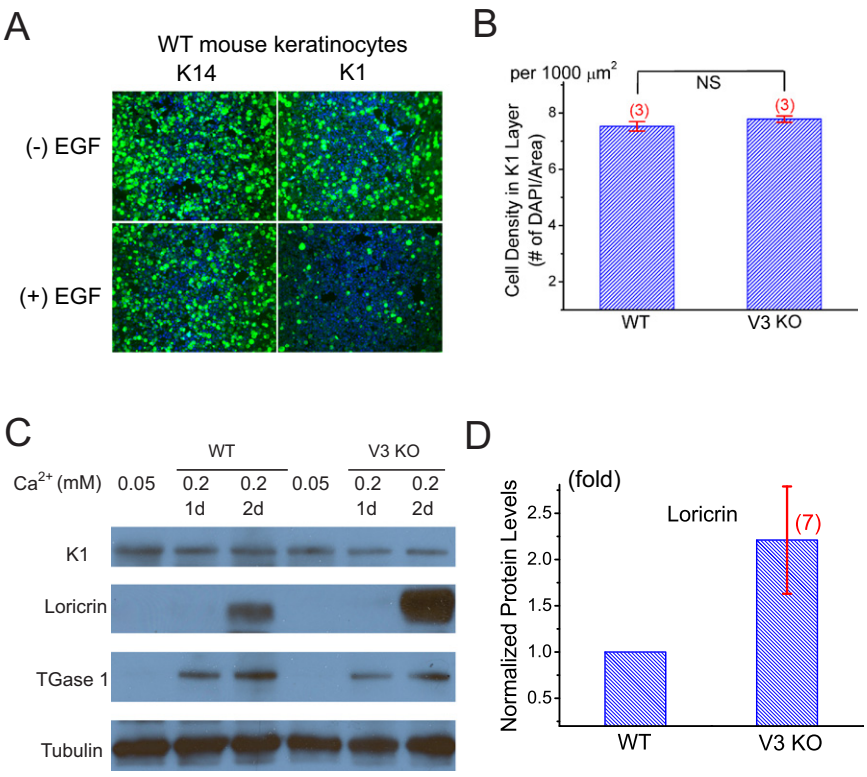

Figure S5. Expression of Early Epidermal Differentiation Markers Is Reduced by EGF but Increased in TRPV3-Deficient Cells, Related to Figure 5

(A) EGF reduces K1 expression in cell-matrix interaction-disrupted keratinocytes cultured in vitro. Immunofluorescence analyses of K14 and K1 were performed after keratinocytes were cultured for 48 hr in suspension.

(B) Normal cell size in the K1-positive layer of V3 KO epidermis. Cell densities of K1-positive layer in WT and V3 KO mice were similar. Cell densities were estimated from the number of DAPI-stained nuclei divided by the area.

(C and D) Cultured V3 KO primary keratinocytes express more early differentiation markers. (C) Immunoblotting analyses of various differentiation markers in lysates from cultured primary keratinocytes. Differentiation was induced by adding 0.2 mM Ca^{2+} to the culture medium (Ca^{2+} switch) for 1 or 2 days. Expression of loricrin was significantly increased in V3 KO keratinocytes. (D) Average increase of loricrin expression in V3 KO keratinocytes.

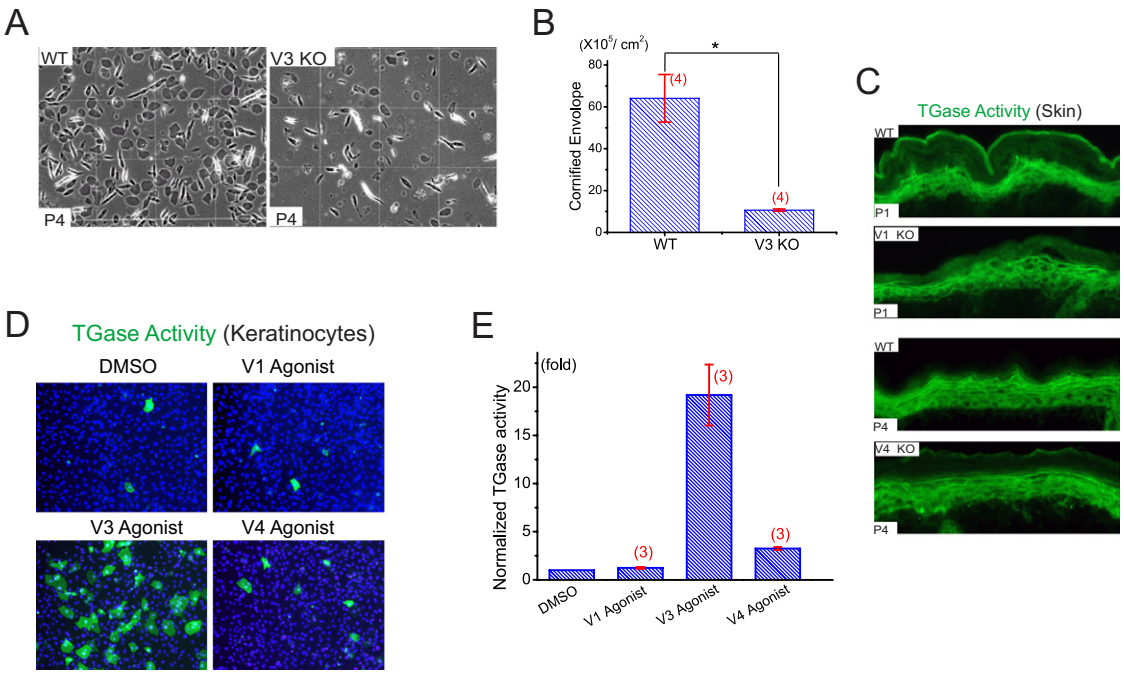

Figure S6. Differential Roles of TRPV1, TRPV3, and TRPV4 in Cornified Envelope Formation and Regulation of TGase Activity, Related to Figure 6

(A and B) Defective cornified envelope formation in TRPV3 global KO mice. Compared to WT littermate pups (P4), the cornified cell envelopes (CEs) of skins of V3 KO pups were significantly less mature.

(C) Comparable TGase activity in the frozen skin sections of neonatal (P1 and P4) WT, V1 KO (P1), and V4 KO (P4) mice. TGase activity was detected using an immunofluorescence-coupled in situ enzymatic assay. Positive staining was restricted to the granular layer of the epidermis.

(D and E) Differential roles of TRPV1, TRPV3, and TRPV4 in CE formation. (D) The effects on TGase activity in WT primary cultured keratinocytes by 40 min application of V1 agonist (1 μM Capsaicin), V3 agonist cocktail (50 μM 2-APB + 200 μM Carvacrol), and V4 agonist (10 μM 4α-PDD). (E) V3 agonist cocktail induced an ~20-fold increase of TGase activity in WT keratinocytes. Whereas V1 agonist induced no significant change of TGase activity, V4 agonist induced a modest but significant (~3 fold) increase of TGase activity.